Lipid remodeling in phytoplankton exposed to multi-environmental drivers in a mesocosm experiment

Sebastian I. Cantarero[1], Edgart Flores[1], Harry Allbrook[1], Paulina Aguayo[2,3,4], Cristian A. Vargas[3,5], John E. Tamanaha[6], J. Bentley C. Scholz[6], Lennart T. Bach[7], Carolin R. Löscher[8,9], Ulf Riebesell[10], Balaji Rajagopalan[11], Nadia Dildar[1], Julio Sepúlveda[1,5]

[1]Deparment of Geological Sciences and Institute of Arctic and Alpine Research (INSTAAR), University of Colorado Boulder, Boulder, CO 80309, USA
[2]Departamento de Oceanografía, Universidad de Concepción, Casilla 160-C, Concepción, Chile
[3]Department of Aquatic System, Faculty of Environmental Sciences & Environmental Sciences Center EULA Chile, Universidad de Concepción, Concepción 4070386, Chile
[4]Institute of Natural Resources, Faculty of Veterinary Medicine and Agronomy, Universidad de Las Américas, Sede Concepcion, Chacabuco 539, Concepcion 3349001, Chile
[5]Millennium Institute of Oceanography (IMO), Universidad de Concepción, Concepción 4070386, Chile
[6]Laboratory for Interdisciplinary Statistical Analysis, Department of Applied Mathematics, University of Colorado, Boulder, Boulder CO, 80309, USA
[7]Institute for Marine and Antarctic Studies, University of Tasmania, Hobart, TAS 7004, Australia
[8]Nordcee, Department of Biology, University of Southern Denmark, Odense, Denmark
[9]Danish Institute for Advanced Study, University of Southern Denmark, Odense, Denmark
[10]Marine Biogeochemistry, GEOMAR Helmholtz Centre for Ocean Research Kiel, Düsternbrooker Weg 20, D-24105, Kiel, Germany
[11]Department of Civil, Environmental, and Architectural Engineering, University of Colorado-Boulder, Boulder, CO, USA

Correspondence to: Sebastian I. Cantarero (sebastian.cantarero@colorado.edu)

Abstract. Lipid remodeling, the modification of cell membrane chemistry via structural rearrangements within the lipid pool of an organism, is a common physiological response amongst all domains of life to alleviate environmental stress and maintain cellular homeostasis. Whereas culture experiments and environmental studies of phytoplankton have demonstrated the plasticity of lipids in response to specific abiotic stressors, few analyses have explored the impacts of multi-environmental stressors at the community-level scale. Here, we study changes in the pool of intact polar lipids (IPLs) of a phytoplanktonic community exposed to multi-environmental stressors during a ~2-month long mesocosm experiment deployed in the eastern tropical South Pacific off the coast of Callao, Perú. We investigate lipid remodeling of IPLs in response to changing nutrient stoichiometries, temperature, pH, and light availability in surface and subsurface water-masses with contrasting redox potentials, using multiple linear regressions, classification and regression trees, and random forest analyses. We observe proportional increases of certain glycolipids (namely mono- and di-galactosyldiacylglycercols; MG and DG, respectively) associated with higher temperatures and oxic conditions, consistent with previous observations of their utility to compensate for thermal stress, and their degradation under oxygen stress. N-bearing (i.e., betaine lipids and phosphatidylethanolamine; BL and PE) and non-N-bearing (i.e., MG, phosphatidylglycerol, and sulfoquinovosyldiacylglycerol; PG, SQ) IPLs are anti-correlated, and have strong positive correlations with nitrogen repleted and depleted conditions, respectively, which suggests a substitution mechanism for N-bearing IPLs under nitrogen limitation. Reduced CO_2(aq) availability and increased pHs are associated with greater proportions of DG and sulfoquinovosyldiacylglycerol (SQ) IPLs, possibly in response to the lower concentration of [$CO_{2(aq)}$] and the overall lower availability of inorganic carbon for fixation. A higher production of MG in surface waters corresponds well with their established photoprotective and antioxidant mechanisms in thylakoid membranes.The observed statistical relationships between IPL distributions, physicochemical parameters, and the composition of the phytoplankton community, suggest evidence of lipid remodeling in response to environmental stressors. These

Deleted: Notable responses include theW
Deleted: uitility
Deleted: high
Deleted: is
Deleted: increased
Deleted: concentrations
Deleted: related
Deleted: for phot
Deleted: osynthesis and biomass production
Deleted: Hh
Deleted: physicochemicalal
Deleted: /chemical
Deleted: Our results
Deleted: trends in
Deleted: L

physiological responses may allow phytoplankton to reallocate resources from structural or extrachloroplastic membrane lipids (i.e., phospholipids and betaine lipids) under high-growth conditions, to thylakoid/plastid membrane lipids (i.e., glycolipids and certain phosphatidylglycerols) under growth-limiting conditions. Further investigation of the exact mechanisms controlling the observed trends in lipid distributions are necessary to better understand how membrane reorganization under multi-environmental stressors can affect the pools of cellular C, N, P, and S, as well as their fluxes to higher trophic levels in a marine environment subjected to increasing environmental pressure. Our results suggest future studies addressing the biogeochemical consequences of climate change in the Eastern Tropical South Pacific Ocean must take into consideration the impacts of lipid remodeling in phytoplankton.

1 Introduction

The Eastern Tropical South Pacific (ETSP) is one of the most productive eastern boundary upwelling systems in the world (Chavez and Messié, 2009) and harbors one of the largest oxygen deficient zones (ODZs) (Fuenzalida et al., 2009; Ulloa and Pantoja, 2009; Thamdrup et al., 2012). Global warming has led to the expansion of ODZs over the recent decades and they are expected to continue expanding due to the reduction in oxygen solubility with increasing temperature (Stramma et al., 2008; Stramma et al., 2010; Gilly et al., 2013), as well as because of enhanced ocean stratification and reduced ventilation of the ocean's interior (Keeling et al., 2010). The future behavior of the ETSP upwelling system in a warmer world remains uncertain; increases in wind-induced upwelling intensity and duration (Gutiérrez et al., 2011; Bakun et al., 2010) may increase the supply of nutrients to the surface in coastal regions, whereas enhanced thermal stratification may reduce nutrient supply in the open ocean (Behrenfeld et al., 2006). Furthermore, upwelling regions are prone to highly variable pH (Capone and Hutchins, 2013), and the global ocean will experience a decreasing average pH as more CO_2 accumulates in the atmosphere and is absorbed by the ocean (Jiang et al., 2019). Accordingly, major shifts in marine planktonic community composition, turnover rates (Henson et al., 2021), and adaptations (Irwin et al., 2015) are expected in future scenarios of ocean conditions, which are expected to lead to cascading effects on ocean biogeochemistry and marine ecosystems (Hutchins and Fu, 2017).

Primary productivity in the ETSP is predominantly regulated by the wind-induced upwelling of nutrients, light availability, and Fe limitation (Messié and Chavez, 2015). Thus, changes in the supply of inorganic N along the upwelling region of the ETSP are likely to induce significant shifts in the phytoplankton community composition. Longer upwelling seasons along nearshore environments could further stimulate productivity of fast-growing eukaryotic algae that currently dominate these systems (e.g., diatoms; Messié et al., 2009). However, shorter upwelling seasons or weaker upwelling currents could favor more survivalist or mixotrophic algae, in addition to N-fixing diazotrophs that thrive under widespread nitrogen limitation (Dutkiewicz et al., 2012). The rate of primary productivity in the surface ocean not only affects the supply of sinking organic matter and thus oxygen consumption via microbial respiration in the subsurface (Wyrtki, 1962), but also results in a shift of redox potentials that drive substantial losses of bioavailable N under reducing conditions at intermediate depths (Lam et al., 2009; Wright et al., 2012). Additionally, expected changes in ocean warming and stratification (Huertas et al., 2011; Morán et al., 2010; Yvon-Durocher, 2015), lowered dissolved oxygen concentration (Wu et al., 2012), and decreased pH (Dutkiewicz et al., 2015, Bach et al., 2017), will disrupt phytoplanktonic assemblages differently based on their individual tolerances and

Deleted: indicative represents significant of
Deleted: physiological responses that
Deleted: Ii
Deleted: this
Formatted: Font: Not Bold
Deleted: remodeling system
Deleted: is
Formatted: Font: Not Bold
Deleted: . In addition to
Deleted: how
Deleted: it may influence
Deleted: of biologically relevant elements
Deleted:
Deleted: and
Deleted:
Deleted: as well as their recycling
Deleted: to the dissolved organic matter pool
Deleted: are impacted
Deleted: include the role
Deleted: of
Deleted:
Deleted: ,

physiological plasticity. However, little is known of the physiological adaptations of phytoplankton on a community-level scale in response to multi environmental stressors.

Phytoplankton have been shown to activate several lipid-based physiological mechanisms in response to environmental stimuli (Li-Beisson et al., 2019; Sayanova et al., 2017; Kong et al., 2018). In fact, intact Polar Lipids (IPLs) are a class of membrane lipids characterized by a polar head group typically attached to a glycerol backbone from which aliphatic chains are attached via ester and/or ether bonds (Sturt et al., 2004; Lipp et al., 2008; Schubotz et al., 2009; Van Mooy and Fredricks, 2010). Dominant planktonic lipid classes include phospholipids with a phosphate-bearing polar head group (e.g., phosphatidylcholine PC; phosphatidylethanolamine PE; and Phosphatidylglycerol PG), glycolipids featuring a sugar moiety in the polar head (e.g., monoglycosyldiacylglycerol MG; diglycosyldiacylglycerol DG; sulfoquinovosyldiacylglycerol SQ), and betaine lipids with a quaternary amine positively charged and attached to lipid chains (e.g. diacylglyceryl hydroxymethyl-trimethyl-β-alanine DGTA; diacylglyceryl trimethylhomoserine DGTS; and diacylglycerylcarboxy-N-hydroxymethyl-choline DGCC) (Kato et al., 1996; Rütters et al., 2001; Zink et al., 2003; Suzumura, 2005; Van Mooy et al., 2006). The remodeling of IPLs, the main constituents of cell and organellar membranes, provides numerous physiological adjustments to attenuate environmental stressors impacting phytoplankton (Zienkiewicz et al., 2016). These include nutrient limitation (Van Mooy et al., 2009; Meador et al., 2017; Abida et al., 2015; Wang et al., 2016), homeoviscous regulation in response to changing temperature (Sato et al., 1980; Sinensky, 1974; Neidleman, 1987) and pH (Tatsuzawa and Takizawa 1996; Poerschmann et al., 2004; Guckert and Cooksey, 1990; Jin et al., 2021), or photosynthetic function under varying light availability (Sato et al., 2003; Gašparović et al., 2013; Khotimchenko and Yakovleva, 2005). While IPL distributions in environmental studies are typically used as chemotaxonomic biomarkers that trace the presence and abundance of specific microbial groups (Sturt et al., 2004; Schubotz et al., 2009; Van Mooy and Fredricks, 2010), their distributions have been used in conjunction with additional microbial or geochemical measurements to assess how microbial metabolisms contribute to the chemical environment (Van Mooy et al., 2009; Wakeham et al., 2012; Schubotz et al., 2018; Cantarero et al., 2020). Yet, few studies have explored how multiple environmental drivers impact IPL remodeling at the community level and in time series, and the associated adaptability of phytoplankton to environmental change.

Deleted: to

Lab-based culture experiments have been a major step forward in understanding how lipid remodeling may impact a biogeochemical system (as summarized above). However, a significant challenge remains in contextualizing these findings at the community scale. Conversely, observational studies from direct measurements of natural systems are often logistically limited in temporal scale, and consequently, do not fully capture the dynamics and heterogeneity of biogeochemical conditions. Mesocosms are experimental apparatuses at the interface between controlled culture experiments and environmental observations that allow for the examination of natural systems and entire ecosystems under semi-controlled conditions to explore the impacts of a changing climate and ocean system (Riebesell et al., 2013). Here, we study changes in the composition, diversity, and abundance of phytoplanktonic IPLs in response to changes in the biological, physical, and chemical composition

of a marine ecosystem subjected to semi-controlled conditions in a 2-month long mesocosm experiment off the coast of Perú. We investigate the potential for IPL remodeling amongst phytoplankton in response to multiple environmental stressors including nutrient availability, O_2 concentration, pH, temperature, and light availability to highlight adaptation strategies available to phytoplankton in response to a changing ocean system.

2 Methods

2.1 Mesocosm Deployment and Sampling

On February 22, 2017, eight "Kiel Off-Shore Mesocosms for Ocean Simulations" (KOSMOS; Riebesell et al., 2013) were deployed just north of Isla San Lorenzo, 6 km off the Peruvian coastline (12.0555º S, 77.2348º W; Fig. 1; Bach et al., 2020) in waters 30 m deep. Each individual mesocosm consisted of a cylindrical polyurethane bag (2 m diameter, 18.7 m length, 54.4 ±1.3 m^3 volume) suspended in an 8 m tall flotation frame. Water exchange was permitted via nets (mesh size 3mm) for three days before the water mass inside each mesocosm was enclosed and isolated from the surrounding Pacific water by attaching sediment traps at the base (~19 m length total). The enclosing of the mesocosms marked the start (day 0) of the 50-day experiment. As detailed in Bach et al. (2020), the experiment involved several manipulations including the addition of ODZ water to simulate upwelling conditions, salt to maintain water stratification, and the introduction of organisms.

The collection of subsurface waters and their addition to the mesocosms is described with detail in Bach et al. (2020). Briefly, on experiment days 5 and 10, two batches of local subsurface ODZ water were collected from stations with varying nutrient stoichiometries (Table 1; Fig. 1) using deepwater collectors first reported by Taucher et al., (2017). The water mass collected from 30 m deep at station 1 (12.028323° S, 77.223603° W) was characterized by a very low N:P ratio (Table 1), whereas the water collected from 70 m deep at station 3 (12.044333° S, 77.377583° W) was characterized by a higher but still low N:P ratio (Table 1). On experiment day 8, 9 m^3 of water was removed from each mesocosm at a depth between 11 and 12 m and then on day 11, 10 m^3 of ODZ water was injected into each mesocosm at depths between 14 and 17 m. On experiment day 12, the entire procedure was repeated but this time with 10 m^3 removed between 8 and 9 m, and 12 m^3 added evenly between 1 and 9 m. To maintain stratification and preserve the low O_2 subsurface layer, a NaCl brine solution was injected evenly into the subsurface of all mesocosms on experiment day 13 (0.067 m^3, 10 to 17 m depth) and experiment day 33 (0.046 m^3, 12.5 to 17 m depth). On day 14, Peruvian Scallop larvae (*Argopecten purpuratus*) were added (~10,000 individuals m^{-3}), and on day 31 Fine Flounder eggs (*Paralichthys adspersus*) were added (~90 individuals m^{-3}). However, few scallop larvae and no fish larvae were found in the mesocosms after the release indicating that their influence on the plankton community was likely small (Bach et al., 2020).

Deleted: ~30 m water depth

Deleted: ;

We sampled two integrated water depths of the mesocosms for suspended organic matter and biological and chemical characterization using 5 L integrating water samplers (IWSs; Hydro-Bios, Kiel) equipped with pressure sensors to collect water evenly within a desired depth range. The samples were collected across two integrated intervals of the water column representing surface and subsurface layers, sampling depths were slightly modified over the course of the experiment to accommodate for changes in water stratification and the position of the chemocline (refer to Bach et al., 2020 for further details). The depths applied for surface and subsurface waters were 0–5 and 5–17 m on days 1 and 2, 0–10 and 10–17 m from day 3 to 28, and 0–12.5 and 12.5–17 m from day 29 to 50.

Samples of suspended organic matter for IPL analysis were collected from all 8 mesocosms at both the surface and subsurface sampling depths on non-consecutive days throughout the experiment. See details of changes in water depths above. Due to the labor- and time-intensive nature of IPL analysis, we focused on 4 mesocosms (two from each treatment) at both depths and from 9 different days spanning the 50-day experiment. We filtered 5 L of mesocosm water through pre-combusted, 142 mm Advantec glass fiber filters (GF75142MM) of 0.3 µm pore size. All samples were wrapped in combusted aluminum foil and shipped frozen to the Organic Geochemistry Laboratory at the University of Colorado, Boulder for IPL extraction and analysis.

2.2 Water Column Physicochemistry

Depth profiles of salinity, temperature, O_2 concentration, photosynthetically active radiation (PAR), and chlorophyll a (chl-a) fluorescence were measured through vertical casts using the CTD60M sensor system (Sea & Sun Technology). O_2 concentrations were cross-verified with the Winkler O_2 titration method performed via a micro-Winkler titration method described by Arístegui and Harrison (2002). Seawater pH_T (pH on total scale), was determined spectrophotometrically using m-cresol purple (mCP) indicator dye as described in Carter, et al. (2013); see Chen et al. (2022) for details. See Bach et al. (2020) for additional detailed information of sampling methods for water column physicochemistry.

Samples for inorganic nutrients were filtered immediately upon arrival at the laboratories at the Instituto del Mar del Perú (IMARPE) using 0.45 µm Sterivex filter (Merck). The subsequent analysis was carried out using a continuous flow analyzer (QuAAtro AutoAnalyzer, SEAL Analytical) connected to a fluorescence detector (FP-2020, JASCO). The method for analyzing PO_4^{3-} followed the procedure outlined by Murphy and Riley (1962), while $Si(OH)_4$ was analyzed according to Mullin and Riley (1955). NO_3^- and NO_2^- were quantified through the formation of a pink azo dye as established by Morris and Riley (1963) and additional corrections to all colorimetric methods was achieved with the refractive index method developed by Coverly et al. (2012). Ammonium concentrations were determined fluorometrically following the method of Kérouel and Aminot (1997). Further methodological specifics and the respective limits of detection for each analysis can be found in Bach et al. (2020).

2.3 CHEMTAX Analysis

Pigment samples were flash-frozen in liquid nitrogen directly after filtration and kept frozen on dry ice during transport to Germany for extraction as described by Paul et al. (2015). Concentrations of extracted pigments were measured by reverse-phase high-performance liquid chromatography (HPLC; Barlow et al., 1997) calibrated with commercially available standards. The relative contribution of distinct phytoplankton taxa was calculated with CHEMTAX, a program for calculating the taxonomic composition of phytoplankton populations (Mackey et al., 1996). Input pigment ratios specific to the Peruvian upwelling system, determined by DiTullio et al. (2005) and further described by Meyer et al. (2017), were incorporated in these calculations (see Bach et al., 2020).

2.4 Flow Cytometry

Samples (650 µL) from each mesocosm were analyzed using an Accuri C6 (BD Biosciences) flow cytometer. The signal strength of the forward light scatter was used to distinguish phytoplankton groups, in addition to the light emission from red fluorescence of chl-a, and the light emission from orange fluorescence of phycoerythrin. Size ranges were constrained via gravity filtration using sequential polycarbonate filters ranging from 0.2 to 8 µm and the strength of the forward light scatter signal. Additional details of this method can be found in Bach et al., 2017. In this study, we only report *Synechococcus* (0.8-3 µm) counts (cells mL^{-1}) because it is the only phytoplankton group that was consistently selected to exhibit statistically significant trends with IPLs likely due to the non-size fractionated nature of IPL sampling.

2.5 Lipid Extraction and Analysis

Intact polar lipids were extracted from glass fiber filters via a modified version (Wörmer et al., 2015) of the original Bligh and Dyer Extraction method (Bligh and Dyer, 1959). Samples were extracted by ultrasonication a total of five times, with three different extraction mixtures. Two extractions were performed using Dichloromethane:Methanol:Phosphate buffer (aq) [1:2:0.8, *v:v:v*], adjusted to a pH of ~7.4, followed by another two extractions using Dichloromethane:Methanol:Trichloroacetic acid buffer(aq) [1:2:0.8, *v:v:v*], adjusted to a pH of ~2.0. A final extraction was performed with Dichloromethane:Methanol [1:5, *v:v*]. After each addition, samples were vortexed for 30 s, sonicated for 10 min, and then centrifuged for 10 min at 3000 rpm while kept at 10 °C. The supernatant of each extraction mixture was then transferred to a separatory funnel where the organic fractions were washed and combined before solvent removal under a gentle N_2 stream. Before analysis, the TLEs were resuspended in dichloromethane:methanol (9:1 *v:v*) and filtered through a 0.45 µm polytetrafluoroethylene (PTFE) syringe filter.

Chromatographic separation and identification of IPLs was achieved using a Thermo Scientific UltiMate 3000 high-performance liquid chromatography (HPLC) interphase to a Q Exactive Focus Orbitrap-Quadrupole high resolution mass spectrometer (HPLC-HRMS) via heated electrospray ionization (HESI) in positive mode, as described in detail in applications

by Cantarero et al. (2020) and Flores et al. (2022). Briefly, a flowrate of 0.4 ml/min was applied to an Aquity BEH Amide column (150 mm, 2.1 mm, 1.7 µm) using a gradient program first described by Wörmer et al (2013). All filtered TLEs were suspended in Dichloromethane:Methanol (9:1, v/v) prior to injection (10 µL) on column. The following HESI conditions were applied; auxiliary gas temperature: 425 °C, capillary temperature 265 °C, spray voltage 3.5 kV, sheath gas flow rate: 35 arbitrary units (AU), auxiliary gas flow 13 AU, S-Lens RF level 55 AU. Samples were analyzed in full scan mode to obtain an untargeted screening (or lipidomic profile) of each sample, in addition to targeted MS/MS mode for compound identification via diagnostic fragmentation patterns (e.g., Sturt et al., 2004; Schubotz et al., 2009; Wakeham et al., 2012). IPLs were identified by their exact masses, polar head groups, the total number of carbon atoms and unsaturations in the core structure, and their retention times. While other studies have analyzed IPLs under both positive and negative ionization modes to determine the composition of individual fatty acid chains in the core lipid structures, we took advantage of the high resolution of the Orbitrap mass spectrometer to focus on the diversity of head group combinations with total carbon atoms and unsaturation only (Cantarero et al., 2020).

Quantification of IPLs was achieved using a combination of an internal standard added (2µg) to samples during extraction (C16 PAF, Avanti Lipids), in addition to an external calibration curve consisting of 17 standards representing different IPL classes (see Cantarero et al., 2020 for full details of all internal/external and deuterated standards). The intensity of each individual IPL identified in the HPLC-HESI-HRMS analysis was calibrated to a linear regression between peak areas and known concentrations of the same lipid class (or the most similar molecular structure) across a 5-point dilution series (0.0001–10 ng/µl). The detection limit, based on individual calibration curves, was determined to be 0.01 ng on column except for DGTS (0.001 ng) and DG, MG, and SQ classes (0.1 ng). Samples were analyzed across 3 separate analytical periods with weekly calibration curves to account for variation in the ionization efficiency of compounds over time. Overall, HPLC-ESI-HRMS is considered a semi-quantitative method due to changes in ionization efficiency of different IPL standards and environmental analytes. These changes are largely caused by differences in polar head group compared to the acyl chain length and degree of unsaturation (Yang and Han, 2011). Nonetheless, we investigate both relative (%) and absolute IPL abundances to compensate for the current analytical limitations in IPL quantification.

Deleted: u

While we report IPL structural variations associated with different head groups and modifications in the core structure (i.e., unsaturation degree and carbon length of diacyl chains), we particularly focus on the former. Additionally, several IPLs thought to be absent in eukaryotic phytoplankton or far more abundant in bacteria and archaea (n = 34 in total) have been removed to facilitate the analysis of trends that are predominantly phytoplanktonic in origin. These compounds include PME/PDME (Phosphatidyl(di)methylethanolamine) and intact GDGTs (glycerol dialkyl glycerol tetraethers) classes. In addition, while we lack detailed structural information of core individual fatty acids, their combined carbon atoms can be used to deduce short (i.e. < 14 carbon atoms per chain) or odd numbered fatty acid chains typically found in bacteria (Volkman et al., 1989; Volkman et al., 1998; Russell and Nichols, 1999; Jónasdóttir, 2019). Thus, compounds conventionally regarded as bacterial (34 in total)

were also removed to minimize their impact on the analysis of predominantly phytoplanktonic IPLs (165 in total). We recognize that while this selection approach reduces the influence of non-eukaryotic lipids, we still cannot rule out an undetermined contribution from heterotrophic bacteria to the IPL pool in this experiment. A summary of these IPL classes and their acronyms is provided in Table 2.

2.6 Multiple Linear Regression

We performed multiple linear regression between 8 relevant environmental factors and 165 unique IPLs. With so many IPL-environmental factor pairs to analyze, we used multiple linear regression (MLR) for quick and easily digestible outputs. In each MLR model, the relative abundance of individual IPL molecules was employed as a response variable, with environmental factors serving as predictor variables. Additionally, phytoplankton abundances were included to account for their linear effects on IPL distributions. The rationale behind this inclusion lies in the understanding that variations in phytoplankton abundance may exert a proportional and predictable impact on the abundance patterns of specific IPLs.

We prioritized linear relationships with IPL relative abundances (% abundances) to emphasize changes in the proportions of phytoplankton lipids, rather than their absolute concentration and contribution to biomass. This approach enables us to distinguish compositional changes in the lipid pool from variability in total biomass production. Additionally, MLRs were constrained to focus on the most abundant IPLs in this system, defined as those constituting more than 2.5% to the total IPL pool. This restriction was implemented to reduce noise associated with low-abundance IPLs and enhance the robustness of analysis.

We chose to investigate linear relationships within individual depths (surface and subsurface) to focus on temporal changes within distinct environments, rather than comparing these two environments directly (see CART and Random Forest methods, below). IPLs and environmental factors were permuted to tabulate the regression coefficient for each IPL-environmental factor pair. Model coefficients were directly comparable due to centering and scaling of environmental and phytoplankton variables (see eq. 1) to linearize the relationship and better align with the model assumptions:

$$Y = \beta_0 + \beta_1 X_1 + \beta_2 X_2 + ... + \beta_n X_n + \varepsilon \qquad \text{eq. (1)}$$

where, Y is the dependent variable (or response), $X_1, X_2, ..., X_n$ are the predictor variable (or independent variables), β_0 is the intercept (constant term), $\beta_1, \beta_2, ..., \beta_n$ are the coefficients representing the magnitude and direction of the relationship between the predictor variable and the dependent variable, and ε is the error term capturing the variability not explained by the model.

Correlations in the MLR analysis were also controlled for false discovery rate following the procedure of Benjamini and Hochberg, (1995) to calculate adjusted p-values and by applying an alpha cutoff of 0.1.

2.7 Classification and Regression Tree (CART) and Random Forest

Classification and Regression Trees (CART; Breiman et al., 1984) are predictive machine learning algorithms that partition and fit data along a predictor axis into homogenous subsets of the dependent variable. Regression trees are used for dependent variables with continuous values, while classification trees for categorical values. Here, we apply regression trees to diagnose the environmental and biological variables that affect IPL concentrations by polar head group class. We limited the size of the tree splits via a "pruning" process, where less significant variable splits are removed as determined by a deviance criterion resulting in the best-fit tree with the least mean squared error. Additionally, predictor variables were selected in conjunction with random forest analyses, which ranks the variable contribution to the model performance.

Random forests are derived from bootstrapping of observational data, and the generation of many decision trees based on each bootstrap sample. We employed a total of 72 samples for the random forest analysis which was run separately for each major IPL class (n = 7) to identify the most important environmental predictors (n = 12) for each individual class of lipid. The random forest method utilizes bootstrap aggregation to generate and average numerous permutations of an out-of-bag score in predictive performance. This approach offers an effective methodology for analyzing high-dimensional data with limited sample sizes (Biau and Scornet, 2016). This method has been widely adopted across various disciplines within the water sciences (Tyralis, 2019), ecological and species distribution modeling (Luan et al., 2020), as well as in bioinformatics and high-throughput genomics (Chen and Ishwaran, 2012; Boulesteix et al., 2012). For a covariate vector, the predicted estimate of IPL class concentrations is an average of the many randomly configured decision trees with the same distribution. A randomly generated subset of decision trees is used to split each node, enabling reduced variance and correlation amongst individual trees, and ideally improving the accuracy of model predictions (Breiman, 2001). The random forest algorithm also allows for the ranking of predictor variables based on the prediction performance and is reported here as the predictor's contribution in reducing the root mean square error (RMSE) in the model. For additional details on the random forest algorithm, please see Hastie et al. (2009). All CHEMTAX, flow cytometry, and physicochemical variables were included in the CART and random forest analyses as predictors. Regression tree (CART) splitting criteria are determined by evaluating the sum of squared deviations in all possible splits and selecting those that result in the greatest reduction of residual error. To prevent overfitting in the CART analysis, a pruning procedure is run to remove nodes that contribute little to the model accuracy based on a cost complexity measure. This procedure allows us to simplify the CART results and thus focus our interpretations on the most significant predictors of IPL headgroups only. In the Random Forest model, following the averaged cross validated accuracy estimates, we implemented a cutoff of 5% reduction in RMSE to eliminate variables that do not significantly reduce

Deleted: It is

Deleted: In order t

Deleted: to

the error of the model prediction. This cutoff allows us to focus our interpretation of only variables that contribute significantly to the out of bag predictor performance (For further details, refer to Supplementary Material, Note S1).

CART and random forest-based predictions serve as ideal methods to explore environmental drivers of IPL distributions- not only because of their predictive performance- but also because of their non-parametric nature, their diagnosis of variable importance, and their ability to handle non-linear interactions and small sample sizes (Tyralis et al., 2019). We do not employ these methods to predict the concentration of IPL classes, but rather to identify the primary environmental and biological drivers of change in IPL class concentrations, and potential interactions between environmental conditions and IPL remodeling amongst phytoplankton. Therefore, we focus our interpretations of both the CART and Random Forest analyses on only the most significant predictors and their relative order of importance in the model predictions.

Deleted: The model variables were reduced via repeated random forest analyses to only include predictors that reduce the RMSE of the model predictions by at least 5%.

Deleted: ¶

3 Results

3.1 Oxygen and pH_T

Oxygen concentration in surface waters ranged between ~125 and 140 µmol/L before the ODZ water addition in all 4 mesocosms (Fig. 2A). The concentration dropped slightly (~15 µmol/L) following the water addition and steadily increased to a maximum between ~185-220 µmol/L by day 28. Day 30 marked a significant drop in oxygen concentration by 30-60 µmol/L in all mesocosms with conditions stabilizing between 140 and 155 µmol/L by day 50. The temporal variability in pH_T in surface waters showed a largely mirrored trend to that of oxygen content. Before ODZ water addition pH_T was 7.9-8.0, which dropped by ~0.2 immediately following the water addition. After a few days of relatively stable pH_T at ~7.8 in all four mesocosms, the pH_T increased significantly between days 18 and 28 reaching ~8.1-8.2. From days 30-40 the pH_T gradually decreased by approximately 0.2 in all mesocosms until increasing again (most notably in mesocosms 7 and 5) between days 42-50 to maxima ranging from 8.1-8.3.

The subsurface waters were more oxygen-depleted compared to the surface and showed an earlier onset of increasing oxygen concentration, beginning immediately after the ODZ water addition. All four mesocosms reached maximum O_2 levels (60-75 µmol/L) by day 13 and began decreasing markedly by day 16. The lowest concentrations (~15 µmol/L O_2) were reached between days 30 and 34. Oxygen concentrations recovered slightly in the last 10-16 days of the experiment and were all within 30 (± 10) µmol/L of O_2. The subsurface waters, again, showed similar temporal patterns in pH_T as with O_2, except for mesocosm 7. The pH_T was variable (~7.60 ±0.05) in the early portion of the experiment (days 10-16) but did not show a dramatic response to the OMZ water addition as was the case in the surface samples. The pH_T did gradually decrease from days 18-30, with pH_T minima in all four mesocosms reached on day 30 (~7.45-7.50). Day 30 also marked the beginning of a significant increase in the pH_T (~0.15-0.20) across all mesocosms with the pH_T steadily increasing to ~7.65-7.70 by day 50. Additional details on the carbonate chemistry of the mesocosms can be found in Chen et al. (2022).

3.2 Nutrient Concentrations

In mesocosm surface waters, the nutrients NH_4^+, NO_3^-, NO_2^-, PO_4^{3-}, and $Si(OH)_4$ all showed consistent trends over time, with the highest concentrations occurring either just before (day 10) or immediately after (day 12) the ODZ water addition (Fig. 2B). Nitrogen species ranged between 1 and 3 µmol/L during this early part of the experiment, while $Si(OH)_4$ ranged between 4 and 7 µmol/L, and PO_4^{3-} remained at ~ 2 µmol/L. The concentration of all nitrogen species dropped quickly to near minimum values by day 15, and typically remained <0.5 µmol/L for the remainder of the experiment. PO_4^{3-} remained replete (>1.5 µmol/L for the entirety of the experiment). $Si(OH)_4$ dropped to ~3-4 µmol/L by day 15 and gradually increased in all 4 mesocosms by 1-2 µmol/L until days 36-38, where concentrations gradually dropped to near minimum values of 3-4 µmol/L. There were periodic enrichments in NH_4^+, most notably between days 40-50, as discussed in Bach et al., 2020.

The mesocosm subsurface water nutrients showed similar temporal patterns as the surface but were generally more enriched in all nutrient species. All nitrogen species decreased in the few days following the ODZ water addition, but at a more gradual pace than in the surface. Before and immediately after the water addition, NO_3^- was enriched at 4-6 µmol/L and NH_4^+ between 2.5-4 µmol/L. NO_2^- concentrations were ~0.5-1 µmol/L in mesocosms 6 and 7 during this period but remained low (<0.3 µmol/L) in mesocosms 5 and 8. Broadly speaking, the nitrogen species all reached minimal values (<0.1 µmol/L) by days 18-20, except for in mesocosms 6 and 8, where NO_3^- persisted at significant concentrations (0.2-2.3 µmol/L) until days 22 and 24, respectively. The remainder of the experiment was marked by typically depleted concentrations of all nitrogen species (<0.1 µmol/L) with occasional spikes in NH_4^+ reaching up to 1 µmol/L, particularly towards the end of the experiment. Subsurface PO_4^{3-} concentrations were similar to the surface, remaining around ~2.0 µmol/L for most of the experiment which gradually decreased to concentrations of ~1.5 µmol/L by the end of the experiment. $Si(OH)_4$ similarly decreased from maximum concentrations of 4.0-4.5 µmol/L shortly after the ODZ water addition, and gradually decreased by ~ 1 µmol/L over the course of the experiment.

3.3 Total Chlorophyll a

Chl-a concentrations were highly variable throughout the experiment, particularly in subsurface waters (Fig. 2C). Concentrations were generally more elevated at the surface compared to the subsurface, with values ranging ~2.56-2.96 µg/L on day 10. In all mesocosms, the chl-a concentration increased to ~7.94-14.01 µg/L after the ODZ water addition and through day 20. Day 22 showed a significant drop in chl-a concentrations to between 1.35 and 2.89 µg/L in mesocosms 7, 5, and 8. Chl-a concentrations at the surface remained rather constant until days 36-40, where concentrations rapidly increased until maximum concentrations on days 48-50 (14.0-47.3 µg/L). In subsurface waters, chl-a concentrations were notably lower than in the surface and ranged between 0.58-0.84 µg/L on day 10. After the ODZ water addition, chl-a concentrations increased slightly until day 14, but did not show consistent distributions amongst the 4 mesocosms afterwards; decreases were observed in mesocosms 6, 5, and 8, but an increase in mesocosm 7. Chl-a concentrations increased rapidly on day 22 in all 4 mesocosms

ranging between 4.03 and 8.44 µg/L. While remaining highly variable, the concentrations generally increased after day 24 with a notably abrupt increase between days 40-44 to near maximum values ranging between 2.58-11.3 µg/L.

3.4 Phytoplankton Community Composition

The CHEMTAX based phytoplankton community compositions demonstrated more variability in phytoplankton assemblages in the subsurface samples than in the surface (Fig. 2C). Before the ODZ water addition on day 10, surface waters in all 4 mesocosms showed similar phytoplankton distributions with high relative abundances of Bacillariophyceae, referred to from here on as diatoms (20-45%), Chlorophyceae (15-50%), and Dinophyceae, referred to as dinoflagellates (25-45%). These distributions remained rather similar immediately after the water addition (day 12), but dinoflagellate contributions increased in the following days and ranged from ~20% of the total chl-a pool to up to 75% by day 20. Of note, Cryptophyceae made minor contributions to the chl-a pool aside from days 15-18 in mesocosm 6 where they contributed up to 25%. Dinoflagellates largely dominated the chl-a pool for the remainder of the experiment with moderate blooms of diatoms between days 34-44 in mesocosms 7 and 8.

Subsurface waters exhibited greater variability in the phytoplankton assemblages and a greater contribution of Chlorophyceae, Cryptophyceae, *Synechoccocus*, and diatoms to the chl-a pool than in the surface. Pre-addition waters (day 10) were dominated by diatoms making up >75% of the chl-a pool. In the first few days after the ODZ water addition (days 12-15), the relative abundance of Chlorophyceae increased to 25-45% in mesocosms 6, 5 and 8, whereas Cryptophyceae contributed between 5-15% of the total chl-a. During this period, diatoms continued to dominate mesocosm 7 but decreased gradually from 65 to 15% of the phytoplankton community. Notably, in mesocosm 6, Cryptophyceae contributed a moderate amount to the chl-a pool beginning on day 15 (25%) and gradually increased to 40% by day 20. Mesocosms 7, 5, and 8 increased in Cryptophyceae as well, but were limited to ~10-25%. Similar to surface waters, dinoflagellates dominated the chl-a pool by day 20 and contributed 50-80% of the chl-a pool; however, there was considerably greater variability in dinoflagellate abundance after day 20 in subsurface waters. Chlorophyceae remained a significant contributor for the rest of the experiment typically ranging between 10 and 25% of the phytoplankton relative abundance. In mesocosms 7, 5, and 8 diatoms became the dominant contributor, totaling ~50% of the phytoplankton between days 32 and 44. By the final days of the experiment (days 48-50), dinoflagellates again made up most of the phytoplankton community (60-75%). Pelagophyceae, Prymnesiophyceae, and Cyanophyceae (referred to here as *Synechococcus*), remained minor contributors throughout the entire experiment but showed maximum contributions of <10% in days 10-16. Mesocosm 6 showed a minor contribution (<10%) of *Synechococcus* from days 42-50, and from days 34-42 in mesocosm 7.

3.5 IPL Class Distributions

The IPL distributions throughout the study can be summarized by the relative abundances of different classes determined by their polar head groups. IPL distributions were broadly consistent between mesocosms and treatments during the experiment

but showed significant differences between surface and subsurface waters (Fig. 2D). Glycolipids such as SQ, DG, and MG typically made up ~50-75% of the total IPL pool in the surface, whereas phospholipids such as PC and PG were dominant in the subsurface (~50-75%). The changes in IPL distribution from the surface samples over the course of the experiment were most apparent between days 10 to 12, 20 to 24, and 24 to 38. Day 10 of the experiment marks the sampling period immediately preceding the ODZ water addition and was the only day with a significant fraction of BLs (betaine lipids) in the total lipid pool (ranging from 25-30% in the surface samples). Mesocosms 6 and 8 showed a similar distribution between days 10 and 12 of the experiment with large contributions of SQs (~50%), BLs (~25-30%), and MGs (~20%), while mesocosms 7 and 5 showed considerably more PCs (~25-40%) at the expense of SQs (<10%). In the 2 weeks following the deep-water addition (days 12 to 24), we saw increasing (albeit variable) relative abundances of PGs (from 5 to 50%) and DGs (from 5 to 25%) in surface waters. MGs made up a considerably larger fraction during this time in mesocosm 6 (up to 50%), but were more moderate in mesocosms 7, 5, and 8 (typically ~25%), yet decreased in all mesocosms to <5% by day 24. The final sample days (38 and 50) showed a resurgence of glycolipid contributions, namely in SQs (25-55%) and MGs (5-25%), with moderate contributions of PGs (5-20%) and DGs (5-20%).

In the subsurface samples before the ODZ water addition, mesocosms 6, 7, and 8 showed moderate contributions of MGs (15-25%) which was lower in mesocosm 5 (<5%). There were higher contributions of SQs in mesocosms 6 and 8 (50% and 35%, respectively) than in 7 and 5 (20-25%). Instead, mesocosms 7 and 5 showed a greater contribution of PCs (45-55%). All 4 mesocosms demonstrated some component of PGs ranging from 5-20% of the total IPL pool. The 2 weeks following the ODZ water addition showed highly variable fluctuations between PCs and PGs as the dominant IPL classes, with the contributions of glycolipids (25-40%) and betaine lipids (<5%) remaining consistent. Of note, day 24 marked a consistently low contribution of PCs, which persisted until the end of the experiment. The final sample days (38 and 50) showed similar contributions between MGs, SQs, and PGs that together dominated the total lipid pool.

3.6 Multiple Linear Regressions

We found statistically significant ($p < 0.05$) linear relationships between the relative abundance of individual IPLs and environmental factors (Figure 3). In surface waters, pH_T showed several significant responses towards DGs, MGs, PGs, PEs and SQs. Classes DG, MG, PE and PG showed negative linear relationships with pH_T, SQs (specifically SQ-32:0), however, showed a strong positive linear response to pH_T. In the subsurface, pH_T only imparted significant linear effects towards SQs with a strong negative linear correlation.

The temperature of surface waters showed predominantly positive regression coefficients with several PG, MG, and DG molecules, with inconsistent correlations found in SQs. Whereas some PEs showed significant linear relationships with temperature, their regression coefficients were near 0. Similarly, in the subsurface only 1 IPL structures (SQ 34:3) showed a significant positive linear response but with a regression coefficient near 0.

Deleted: Amongst

Deleted: SQ

Deleted: , there were both positive and negative

Deleted: ;

Deleted: IPLs containing 3 or more unsaturations showed negative relationships, and molecules with fewer than 3 unsaturations showed positive relationships. PG

Deleted: exclusively negative

Deleted: s

Deleted: similar pattern of generally more unsaturations positively related to pH_T

Deleted: and

Deleted: DG and

Deleted: the remaining IPL classes

Deleted: 2

Deleted: DG and

Deleted: s

Oxygen concentrations showed few linear correlations at the surface and were limited to two BLs (negative) and 1 PG (positive). In the subsurface, the strongest linear correlations were found between oxygen and PGs and SQs (negative).

Nutrient concentrations showed many significant linear responses with regression coefficients of higher magnitude (up to ± 8) and adjusted R^2 values of up to 0.5. The concentration of various forms of inorganic nitrogen had largely positive linear responses to BLs and PCs in both the surface and subsurface, with strongly negative responses in PGs and subsurface MGs. Among the SQs, many individual molecular species, with different fatty acid chains, responded linearly to all forms of inorganic N, the signs of these relationships were negative but in the surface, and generally positive in the subsurface (aside from NO_2^-). DGs showed only one positive linear response in the subsurface. PEs showed little response to inorganic nitrogen concentrations (regression coefficients near 0). PO_4^{3-} concentrations showed only a few significant responses from BLs (negative) and PGs (slightly positive) in the surface. However, in the subsurface, PO_4^{3-} showed strong linear responses (negative) to several MG and PG molecules, and strong positive relationships with several PCs.

Light showed few linear responses amongst IPL relative abundances. At the surface, the strongest relationships were amongst PG (positive) and SQ (mixed signs) and to a slight degree BLs (negative). In the subsurface, only one SQ with a significant linear relationship was noted and with a weak regression coefficient, indicating a range of light saturation with little to no linear effect on IPL distributions.

3.7 CART and Random Forest

All the predictive tree-based models showed improved performance with the inclusion of environmental variables (Figs. 4-7). The CART decision trees iteratively identified the key biological and physicochemical variables producing the best performing model in the prediction of IPL concentrations. The random forest analysis compliments these best fit decision trees by calculating the % reduction in the root mean square error (RMSE) associated with each variable. In conjunction, these two analyses highlight the most impactful variables in predicting the concentrations of a given IPL class. Overall, model performance amongst each IPL class can be compared by the strength of the correlation coefficients between observed and predicted concentrations, and by the magnitude of the RMSE (Figs. 4-7).

Amongst several IPL classes (i.e., SQs, DGs, and BLs), pH_T was consistently a significant contributing variable to IPL concentrations, as demonstrated by both the CART and random forest analyses (Fig. 4A-D, and Fig. 5). Notably, pH_T was identified as the most important variable amongst the best fit decision trees for both SQs and DGs, as well as the random forest model for SQs. Oxygen concentration was also frequently identified as a major contributing variable to model performance with MGs, DGs, PEs, PCs, (Figs. 4E-H, 5A-D, 6E-H, and 7A-D, respectively) and moderately important in SQs (Fig. 4A-D).

Deleted: and SQs (mostly negative)

Deleted: Whereas other linear relationships did appear with oxygen, they were comprised of near 0 regression coefficients.…

Deleted: (in the subsurface)

Deleted: - however,

Deleted: inconsistent

Deleted: at depth

Deleted: few

Deleted: s and only

Deleted: , with similarly inconsistent signs

Deleted: -IPLs

Deleted: did not show many

Deleted: aside

Deleted: few

Deleted: s

Deleted: ere

Deleted: none

Deleted: significant

Deleted: s

Temperature was selected as the most important variable in PE predictions (Fig. 6E-H), and a major contributing variable in SQ, MG, BL, PG, and PC predictions (Figs. 4-7). Various forms of biologically available nitrogen were also important in the prediction of MG (Figs. 4E-H), BLs (NH_4^+; Figs. 5E-H), PE (NH_4^+; Figs. 6E-H), and PG (NH_4^+ and NO_2^-; Figs. 6A-D). PO_4^{3-} concentrations showed significant contribution to model performance amongst BLs (Figs. 5E-H, denoted as Si:P ratios), SQs, MGs, PGs, and PEs (Figs. 4A-D, 4E-H, 6A-D, and 6E-H, respectively). Finally, light availability demonstrated secondary but significant importance in the prediction of SQs, MGs, PGs, PEs, and PCs (Figs., 4A-D, 4E-H, 6A-D, 6E-H, and 7 respectively).

Variables indicative of biological abundance were also identified as highly impactful to model performance, with chl-a concentration showing a significant contribution to all lipid classes except BLs (Figs. 4-7). Individual phytoplankton abundances also showed to be important predictive variables such as Cryptophyceae abundances for BLs, dinoflagellate abundances for DGs and SQs, *Synechococcus* abundances for DGs, PCs, PEs, and PGs, and diatoms for PCs.

3.8 Water Treatments

The experiment consisted of applying two different treatments to the mesocosms, aimed at exploring the varying impacts of upwelling of ODZ waters with contrasting geochemical properties. The first treatment saw the introduction of water from a coastal area (station 1) with ODZ waters with a very low N:P ratio (0.1; see Table 1, and Fig 2B) into the mesocosm. The second treatment performed the same process, but with ODZ water from an offshore area (station 3) with a low N:P ratio (1.7; Table 1, and Fig 2B). Despite the different chemical signatures of the added water-masses, the resulting nutrient stoichiometries within the mesocosms were similar in between both treatments, likely due to both dilution effects and the time passed between water collection and addition (see Bach et al., 2020). We see largely similar responses in the IPL distributions, as well as in other biogeochemical variables between these two treatments; therefore, we largely focus our discussion on the temporal variation and differences between surface and subsurface environments in these analyses.

4 Discussion

4.1 Biological Abundances as Drivers of IPL Distributions

We expect phytoplankton abundances to exert first order control on the production and distribution of IPLs in this experiment. The majority of the detected molecules have been demonstrated to be chemotaxonomic biomarkers of planktonic biomass (Sturt et al., 2004, Schubotz et al., 2009, Wakeham et al., 2012; Van Mooy and Fredricks, 2010; Cantarero et al., 2020). Previous work in the Humboldt Current System shows that the ratio of total IPLs to POC is high at the chlorophyll maximum and the composition of IPLs found in these surface waters are consistent with predominantly phytoplanktonic biomass (Cantarero et al., 2020). In this mesocosm experiment, the depths of the chlorophyll maximum and oxycline are compressed into a 20 m water column which likely drives a greater contribution of phytoplanktonic IPLs in ODZ waters than would be expected in the natural environment. While we suggest that most of the biomass (and IPL content) measured at these high

Deleted: both

Deleted: , as

Deleted: these

Deleted: se

chlorophyll depths is likely derived from phytoplankton, we cannot completely isolate nor quantify the contribution of bacterial biomass to the total IPL pool.

Most IPL classes demonstrate phytoplankton abundances as a primary or major predictor in the CART and random forest analyses, such as dinoflagellates in the prediction of SQs (Figs. 4A, C), DGs (Figs. 5A, C), and PE (Fig. 6G), *Synechococcus* in the prediction of PGs (Fig. 6A, C), PEs (Fig. 6E, G), and PCs (Fig. 7A, C), and chl-a in the prediction of every IPL class barring BLs (a mostly minor IPL class in this experiment). Chl-a appears most important in highly abundant IPL classes as an indicator of overall photosynthetic productivity, and dinoflagellates dominate the overall phytoplankton biomass for almost the entirety of the experiment post ODZ water addition. *Synechococcus* demonstrates covariance with the total phytoplankton biomass, yet remains a relatively minor phytoplankton class. We suggest that the prevalence of biological sources as IPL predictors in the decision tree analyses generally indicates the variability in total phytoplankton biomass throughout the experiment.

Among phytoplankton, glycolipids MG, DG, and SQ are predominantly found in thylakoid membranes, whereas phospholipids PC and PE, as well as BLs are structural components in the cell membrane lipid bilayer (note PG is found in both; Guschina and Harwood, 2013). It is important to recognize that the relative proportions of IPLs vary in different phytoplankton classes (Harwood and Jones, 1989; Wada and Murata, 2009), and that many of these lipids, in particular phospholipids, can also be derived from heterotrophic bacterial biomass (Popendorf et al., 2011). Thus, the overall community composition is expected to be a major driver of IPL distributions in this system. However, given the prevalence of algal biomass and the steps taken to minimize bacterial contributions to the IPL pool (see section 2.5), we focus our analysis on that of phytoplanktonic dynamics. We recognize that both phytoplankton abundances and the total planktonic community composition play a major role in the distribution of IPLs. Thus, while the data presented here may refine the phylogenetic association between biological sources and IPLs in marine systems, our main aim is to explore the role of multiple environmental forcing as an additional control on IPL distributions. The following sections focus on the evidence for direct environmental influence on IPL remodeling amongst the phytoplankton community and the potential implications of these physiological responses to broader aspects of ocean biogeochemistry.

4.2 Environmental Variables as Drivers of IPL Remodeling

Since community composition can change concurrently and/or in response to environmental conditions, we employed two distinct strategies to isolate the role of lipid remodeling as a physiological response to environmental forcing only. Firstly, the MLRs which subtract the variability explained by phytoplankton abundance (e.g., CHEMTAX results) in pairwise correlations between lipid abundances and environmental variables. Secondly, the decision tree analyses (CART and Random Forest) which rank variables by their impacts on the model performance.

Deleted: which may still make a significant contribution

Deleted: Indeed, m

Deleted: bility

Deleted: thus its perceived importance in controlling the abundance of several IPL classes is likely due this covariance, as *Synechococcus*

Deleted: G

Deleted: , as well as the relative abundance of each species within the phytoplankton community, are

Deleted: s

Deleted: , h

Deleted: Apart from a minor contribution from cyanobacteria (Fig. 2C) to the chl-a pool (presumably the IPL pool as well), our dataset primarily focuses on photosynthetic eukaryotes. Accordingly,

Deleted: w

Deleted: we

Deleted: se

Deleted: specificity of

Deleted: of

Deleted: the

Deleted: In many cases,

Deleted: s

Deleted: . Therefore,

Across virtually every major IPL class common to eukaryotic phytoplankton we see evidence of environmental conditions exherting significant control on polar headgroup distributions in the MLRs (Fig. 3). Similarly, nutrient concentrations, pH_T, temperature, O_2 concentration, and light availability are consistently identified as statistically important variables in the prediction of IPL head groups in both the CART and Random Forest analyses (Figs. 4-7). In addition, high level comparisons in the relative abundances of IPLs and phytoplankton groups (Figs. 3C, D) suggest that certain environmental conditions may be associated with major shifts in IPL distributions.

An important distinction between the MLRs and the decision trees is that the MLRs are calculated within individual depth environments (surface and subsurface) to explore statistically significant linear relationships between abundant IPL molecules and changing environmental conditions. On the other hand, the decision trees explore the predictive power of physicochemical differences between the surface and subsurface environments on IPL distributions. The results of these two analyses are meant to be complimentary, in that they focus on the differences in environmental conditions between water depths as well as the temporal development of conditions within a given depth over the course of the experiment.

4.2.1 Nutrient Availability

Nutrient limitation amongst phytoplankton leads to transitions in cellular activity, from the biosynthesis of growth/reproduction cellular components such as cell membranes to energy storing molecules (Guschina and Harwood, 2013, Zienkiewicz et al., 2016). Nitrogen, an essential nutrient in photosynthesis and the biosynthesis of proteins/enzymes and nucleic acids, is typically acquired by marine phytoplankton through inorganic nitrogen species such as NO_3^- and NH_4^+. Some phytoplankton can also utilize organic nitrogen sources (Bronk et al., 2007), whereas diazotrophic cyanobacteria can fix dinitrogen gas into bioavailable nitrogen. The coastal region of the ETSP is typically considered to be seasonally co-limited by light, N, and Fe (Messié and Chavez, 2015). However, along the Peruvian shelf Fe concentrations are elevated compared to offshore waters (Hutchins et al., 2002; Browning et al., 2018), and is not considered a limiting source in this mesocosm experiment (Bach et al., 2020). In our mesocosm systems, the inorganic N:P ratio ranged between 0.13 and 4.67, with higher inorganic N in subsurface waters compared to the surface, and with a N:P minimum reached by day 20. Bach et al., (2020) noted that a week after the ODZ water addition, increases in the particulate organic carbon to biogenic silica ratios coincided with low inorganic N and high $Si(OH)_4$ concentrations, suggesting a N-limited system. Thus, we consider our system to be overall nitrogen limited with varying degrees of severity throughout the course of the experiment. This N-limitation is also reflected in the transition from predominantly diatoms, Chlorophyceae, and Cryptophyceae to a dominance of mixotrophic dinoflagellates approximately 4-6 days after the initial ODZ water treatment (Bach et al., 2020). Such shifts are consistent with the ecological advantage that dinoflagellates exhibit under N-limiting conditions as they can extract nitrogen from the dissolved organic nitrogen (DON) pool (Kudela et al., 2010) as well as from heterotrophy (Smalley et al., 2003)

Deleted: forcing

Deleted: IPL

Deleted: physicochemical variables such as

Deleted: are able to

Deleted: m

Deleted: T

Deleted: relatively enriched

Deleted: that

Deleted: this mesocosm

Deleted: -

Deleted: is

Deleted: ir

Deleted: to

Deleted: ecological changes from bloomer to survivalist species associated with cellular resource reallocation (Arrigo, 2005).…

In our study, all four mesocosms experienced limitations in inorganic nitrogen (as low as 0.24 µmol/L) and consistently high concentrations of PO_4^{3-} (ranging from 1.3 to 2.3 µmol/L) throughout the entire experiment. Random forest analysis shows that the inorganic N concentration is an important predictor in the abundance of BL, PG, and MG (Figs. 5G, 6A, and 4E, respectively). The MLRs also indicate that many individual molecules from nearly every IPL headgroup have significant linear correlations with inorganic N concentrations (Fig. 3). Of note, the distributions of several abundant PCs and BLs with N in the headgroup structure are consistently positively correlated with inorganic N species. Whereas other non-N-bearing IPLs are generally negatively correlated with inorganic N concentration (PG, SQ and MG) meaning that they are proportionally more abundant under more severe N-limitation.

Under P limitation, phytoplankton are known to substitute non-phosphorus-containing glycolipids for phospholipids and reallocate the liberated P for other cellular demands (Van Mooy et al., 2009). We hypothesize that non-N-containing glycolipids and phospholipids may similarly be substituted for IPLs such as PCs and BLs as a mechanism for alleviating cellular N demand in low inorganic N conditions. Both PC and BL are found in extra-chloroplast membranes (Kumari et al., 2013), whereas IPLs found in thylakoid membranes such as MG, PG, and SQ are essential to the photosynthetic machinery. Indeed, the average ratio of total IPLs/chl-a is up to three times higher at depth than in surface waters (Fig. S5), possibly pointing towards a reduced proportion of membrane lipids among phytoplankton subject to environmental stressors such as nutrient limitation (likely in addition to oxygen availability, temperature, and light levels). We note that at least a fraction of this trend could also be explained by the contribution of IPLs from heterotrophic bacteria.

More generally, nutrient limitation can cause phytoplankton to accumulate highly concentrated stores of energy in the form of triacylglycerols (TAGs) through the activation of multiple biosynthetic pathways (Zienkiewicz et al., 2016). These include synthesis via acyl units donated from phospholipids via the PDAT (phospholipid:diacylglyceroltransferase) enzyme (Dahlqvist et al., 2000), or other chloroplast membranes, as demonstrated in the homologous enzyme Cr-PDAT (Yoon et al., 2012), as well as several DGAT(diacylglycerol:acyl-CoA acyltransferases; Li et al., 2012; Li-Beisson et al., 2019). These enzymes represent significant pathways for TAG accumulation (Popko et al., 2016; Gu et al., 2021), are sensitive to N availability (Yoon et al., 2012; Li et al., 2012), and their encoding genes have so far been identified in green algae, diatoms, and heterokonts (Zienkiewicz et al. 2016). Because our dataset does not include TAG production, further work on this aspect could reveal whether the proportional changes in dominant phytoplanktonic IPLs correlated to N availability are also associated with TAG synthesis, and if so, determine whether recycling of membrane lipids is a significant contributor to these observed community-level distributions.

Deleted: ,

Deleted:

Deleted: Whereas

Deleted: enzymes associated with the endoplasmic reticulum (Liu and Benning, 2013), de novo TAG synthesis in the chloroplast (Fan et al., 2011), as well as from phospholipids acting as donors of acyl units for TAGs production via the

Deleted: PDAT (phospholipid:diacylglyceroltransferase) enzyme (Dahlqvist et al., 2000). The PDAT enzyme can be a significant pathway for TAG accumulation (Popko et al., 2016; Gu et al., 2021) and the encoding genes have been identified so far in green algae, diatoms, and heterokonts (Zienkiewicz et al. 2016).

Deleted: In our study, all four mesocosms experienced limitations in inorganic nitrogen (ranging from 0.24 and 4.29 µmol/L), and consistently high concentrations of PO_4^{3-} (ranging from 1.3 to 2.3 µmol/L) throughout the entire experiment. While random forest analysis only detected a significant impact of inorganic N concentration amongst BLs, PGs, and MGs (Figs. 5G, 6A, and 4E, respectively), the MLRs also suggest several individual molecules with significant linear relationships amongst PCs and SQs (Fig. 3). Of note, the distributions of several abundant PCs and BLs with N in the headgroup composition are positively correlated with inorganic N species. Other IPLs associated with N availability (PG, SQ, and MG) are generally negatively associated, meaning that they are more abundant under more severe N-limitation.

Deleted: ¶

4.2.2 pH_T and Inorganic Carbon Availability

Coastal upwelling zones are characterized by low pH_T subsurface waters associated with ODZs, where high fluxes of organic substrates sustain enhanced microbial respiration and the accumulation of CO_2 (Capone and Hutchins, 2013). Thus, we explore evidence for membrane lipid remodeling amongst phytoplankton as a physiological response to varying pH_T. We see evidence of pH_T imparting a potential control on the composition of IPL head groups, particularly amongst SQs and DGs, as noted by the high importance rankings in both the CART and Random Forest analyses (Figs. 4A,C and 5A,C). This likely represents the relatively high abundance of these glycolipids in the surface samples where the pH_T is 0.2-0.6 higher than at depth. The MLRs show several negative correlations between MG, PG, and SQ molecules containing unsaturated or polyunsaturated fatty acids with pH_T (Fig. 3). The observed increased proportion of unsaturated IPLs at lower pH_T is most apparent in surface waters where the variability in pH_T is greatest (± 0.2). It has been suggested that lower pH_T can induce greater proportions of saturated fatty acids as a mechanism to reduce membrane fluidity and prevent high proton concentrations in the cytoplasm (Tatsuzawa et al., 1996). However, this response remains limited to more extreme pH_T ranges (e.g., ~1-10), suggesting that other environmental factors (e.g. nutrient availability) are overprinting the potential impacts of pH on fatty acid saturation.

Rather than a direct consequence of modest changes in pH_T on algal membrane fluidity, the observed changes in fatty acid profiles may be in part a response to the available forms of inorganic carbon for photosynthesis. Following the ODZ water addition, DIC (dissolved inorganic carbon) and pCO_2 rapidly declined within a few days (Chen et al., 2022) due to high productivity. In natural waters, pCO_2 maxima occur in ODZ waters where respiration rates are high (Vargas et al., 2021). Lower pCO_2 at the surface may be a limiting factor for photosynthesis and growth; higher pH_T in marine settings indicates a reliance on active transport of HCO_3^- for carbon fixation as opposed to a passive diffusion of CO_2 (Azov et al., 1982; Moazami-Goudarzi et al., 2012). Enrichment of pCO_2 has also been observed to induce an increased proportion of unsaturated fatty acids in microalgae (Morales et al., 2021), which may explain the negative correlation between the proportion of certain unsaturated glycolipids (as well as PGs) and pH_T (high pCO_2; see Fig. 3).

As mentioned above, phytoplankton can employ membrane lipids as substrates for TAG accumulation in phytoplankton under environmental stress. While nutrient limitation is often considered the primary regulator of TAG production, culture experiments also point toward the importance of pH and inorganic carbon availability (Guckert and Cooksey, 1990; Gardner et al., 2011), with different responses between a model diatom (*Phaeodactylum tricornutum)* and chlorophytes (CHLOR1 and *Scenedesmus sp.* WC-1), which is potentially related to individual carbon concentrating mechanisms (Gardner et al., 2012). For instance, under nitrogen/phosphorus limitation, TAG production can be promoted if the supply of inorganic carbon is abundant (Peng et al., 2014). TAGs can also be synthesized and accumulated when inorganic carbon is limited by invoking the recycling of IPLs such as glycolipids and phospholipids (Peng et al., 2014). Thus, the higher proportions of SQs and DGs in the high pH/low $CO_2(aq)$ surface waters of our experiment could be in part related to their recycling under CO_2 limitation.

Deleted: Amongst *Chlamydomonas reinhardtii*, Cr-PD... [1]
Deleted: ¶
Deleted: We suggest that N-bearing IPLs such as PC a... [2]
Deleted: a complex relationship between individual IP... [4]
Deleted: associated with
Deleted: (particularly amongst DG, MG, and to some ... [5]
Formatted ... [3]
Deleted: production of
Deleted: ;
Deleted: h
Deleted: only limited responses have been observed in... [6]
Deleted: amongst *Chlamydomonas sp.* (Poerschmann... [7]
Deleted: .
Deleted: the
Deleted: effects
Deleted: result of
Deleted: other carbonate chemistry parameters in this ... [8]
Deleted: The surface waters afte
Deleted: r
Deleted: showed rapid declines
Deleted: rapidly declined
Deleted: in
Deleted: ,
Deleted: as is typical of the ETSP with
Deleted: whereas
Deleted:
Deleted: r
Deleted: ing
Deleted: the
Deleted: concentrations
Deleted: It has been suggested that elevated CO_2 level... [9]
Deleted: Another possible explanation for the associa... [10]
Formatted ... [11]
Deleted: It has been proposed that
Deleted: even
Deleted: may
Deleted: by
Deleted: abundant
Deleted:
Deleted: to provide substrates for
Deleted: s
Deleted:
Deleted: or
Deleted:
Deleted: polar lipids when inorganic carbon is limited
Deleted: culture experiments of TAG production in ... [14]
Deleted: Additionally, the chlorophyte *Scenedesmus* ... [15]
Formatted ... [12]
Formatted ... [13]

Overall, our results are consistent with other experimental data in that pH_T impacts the distribution of IPL head groups amongst certain phytoplankton groups. For instance, the relatively high glycolipid abundances in surface samples with higher pH_T (most notably SQ and DG, see Fig. S1) are likely not related to direct effects on membrane fluidity, but rather to the availability of inorganic carbon and its effect on the recycling of phospholipids (as well as MGs), potentially for TAG synthesis. While our results are consistent with the so far observed IPL substrates for TAG synthesis (Dahlqvist et al., 2000; Yoon et al., 2012), additional analyses of TAG concentration and their fatty acid compositions amongst the phytoplanktonic community would aid in tracing the extent of membrane lipid degradation as a source of acyl units, as well as to trace the location of these biosynthetic pathways in the cell. Such work would aid in determining the extent to which TAG synthesis and IPL recycling relegates phytoplankton classes to certain depths of the water column based on the combined effects of nutrient availability and pH_T (amongst other variables; e.g. light, temperature, O_2.)

4.2.3 Oxygen

Despite the harvesting of light energy during photosynthesis, photosynthetic organisms also rely on respiration for growth and free radical scavenging under both light and dark conditions (Raven and Beardall, 2003). Specifically, the availability of O_2 (particularly during the dark phases or in low-light environments) influences the activation of metabolic responses, such as fermentative metabolism and acetate utilization (Yang et al., 2015). Differences in dark respiration rates relative to light-saturated photosynthesis among algae may confer advantages under varying oxygen availability (Geider and Osborne, 1989). Thus, the ability of some organisms to perform lipid remodeling in response to oxygen stress may partially shape the composition of the phytoplankton community.

In our analysis, the Random Forest models indicate a significant impact of O_2 concentration in the prediction of nearly all IPL class abundances (Figs. 4-7). This pattern appears to be largely driven by differences in IPL distributions between surface (oxygenated) and subsurface (hypoxic; < ~1.4 ml/L as defined by Naqvi et al., 2010) waters. Glycolipids (MG, DG, and SQ) make up on average 28% more of the IPL pool in the oxygenated surface waters (~125-220 µmol/L O_2) compared to oxygen deficient subsurface waters (~15-75 µmol/L O_2). The MLRs, however, show no significant relationships between individual glycolipid relative abundances and O_2 concentration in surface samples (Fig. 3); this is possibly due to surface waters remaining well oxygenated throughout the experiment. While several IPL moieties found in BLs, SQs, and PGs demonstrate mostly negative linear relationships (Fig. 3), we suggest that the most prominent and consistent relationships are driven by a major shift from oxic to hypoxic conditions (i.e., surface vs subsurface) as opposed to a sensitivity to variable O_2 concentrations.

Commented [1]: RC2-26: L 608-609 – I suggest t... [19]
Deleted: Notably, enhanced TAG production was not... [16]
Deleted: ¶
Deleted: Differences in the effect of carbonate chemi... [17]
Deleted: Based on the dominance of dinoflagellates i... [18]
Deleted: ↵ ... [20]
Deleted: Furthermore, given the dominance of
Deleted: dinoflagellates in surface waters, their abilit... [21]
Deleted: ¶
Deleted: ¶
Deleted: agree
Deleted: may
Deleted: play a significant role in
Formatted ... [22]
Deleted: T
Deleted:
Deleted: CO_2
Deleted: and the concomitant recycling of membrane lipids
Deleted:
Deleted: .
Deleted: A
Deleted: A
Deleted: amongst the phytoplanktonic community
Commented [4]: I think wording in that this is the... [23]
Deleted: to
Deleted: e
Formatted ... [24]
Deleted: Thus, the capability of some organisms to p... [25]
Formatted ... [26]
Formatted ... [27]
Deleted: we posit that this is
Deleted: The deep samples
Deleted: indicate
Deleted:
Deleted: few statistically significant
Deleted: , most notably a negative relationship with s... [28]
Deleted: . This suggests
Deleted: is
Deleted: change
Deleted: and not
Deleted: increasingly depleted
Deleted: Oxygen availability appears to impart a sign... [29]

Anaerobiosis amongst green algae has been demonstrated to impact lipid production, with significant reductions (by nearly 50%) in polar lipid content and concomitant increases in fatty acids (Singh and Kumar, 1992). Gombos and Murata (1991) found that the cyanobacterium *Prochlorothrix hollandica* experienced a significant reduction in the relative abundance of MGs that coincided with moderate increases in SQs, DGs, and PGs under low oxygen conditions. Furthermore, culture experiments of anaerobically grown *Chlamydomonas reinhardtii* resulted in both decreased membrane lipid yields (most notably amongst MGDGs and DGDGs; by > 50%) and an accumulation of TAGs (Hemschemeier et al., 2013). It has been noted that oxygen stress appears to induce the degradation of fatty acids (~30% reduction under dark/anaerobic conditions), mostly amongst unsaturated fatty acids commonly found in MGDG and DGDG membrane lipids (16:4 and 18:3) used for TAG assembly (Liu, 2014; Hemschemeier et al., 2013). Glycolipids (i.e., MG and DG) appear to serve as important substrates for TAG production under low oxygen conditions; however, beta-oxidation of fatty acids requires oxygen to contribute to the degradation of acyl groups, potentially explaining why membrane lipid degradation is attenuated under more severe hypoxia (Liu, 2014). This physiological response to low oxygen conditions in subsurface waters may explain the relatively high abundance of glycolipids in well oxygenated surface waters.

Dinoflagellates have been shown to exhibit particularly high dark respiration to light-saturated photosynthetic rates as compared to diatoms, Chlorophyceae, or most notably cyanobacteria (Geider and Osborne, 1989), possibly pointing towards a greater sensitivity to O_2 concentrations. In addition to other environmental conditions, the greater relative abundance of Chlorophyceae, diatoms, and Cryptophyceae in the oxygen-deficient subsurface waters may reflect reduced respiration rates amongst these algae. Differences in the proportion of glycolipids MG and DG amongst different algae, and their relative ability to recycle them under oxygen stress, may play a prominent role in their individual tolerances to oxygen limitation.

Higher proportions of glycolipids in surface waters may also be due to enhanced rates of microbial degradation under oxic conditions, which may be 2-4 times faster than under anoxic conditions, as tested in microcosm experiments (Ding and Sun, 2005). Relatively labile glycolipids can accumulate in the dissolved organic carbon pool (Gašparović et al., 2013). This observation aligns with the slower breakdown of SQs compared to phospholipids observed in IPL degradation experiments under aerobic conditions (Brandsma, 2011). This accumulation process, however, is unlikely in regions of the water column with large numbers of active living cells, and highly active bacterial degradation. In fact, the distributions of IPLs across the ODZ of the ETSP indicate minor contributions of exported IPLs to greater depths, suggesting high surface recycling (Cantarero et al., 2020). However, specific experimental observations encompassing oxygen gradients ranging from well-oxygenated to fully anoxic conditions are necessary to derive more robust conclusions.

4.2.4 Temperature

Phytoplankton have been shown to respond variably to high growth temperatures depending on their individual tolerances (Huertas et al., 2011). Photosynthesis is considered the most heat-sensitive cellular function in photoautotrophs (Berry and Björkman, 1980). In this section we discuss the potential lipidomic responses to heat stress within the IPL distributions of the phytoplanktonic community. Temperature fluctuations affect membrane fluidity, a phenomenon commonly controlled by fatty acid desaturases (Sakamoto and Murata 2002) that catalyze the production of unsaturated/saturated fatty acids to increase/decrease membrane fluidity, respectively (Lyon and Mock 2014). We did not see evidence for temperature effects on the degree of unsaturation in our data (see Fig. S2). This is likely due to the overall narrow temperature range observed during the experiment (17.3 - 21.6 ºC), which mirrors the natural variability observed in Callao (average monthly ranges ~16.6-19.6 ºC from 2017 to 2019 (Masuda et al., 2023).

Despite the restricted temperature range and its lack of impact on the unsaturation degree of core lipids, the random forest analyses identified temperature as a significant variable in predicting all IPL classes based on their polar head groups aside from DG and PE (Figs. 4-7). This suggests that the response to temperature may vary among different IPLs classes. The MLRs indicate consistently positive relationships between several glycolipids and temperature, suggesting a potential physiological compensation via membrane compositions for higher temperatures. Gašparović et al. (2013) noted an accumulation of glycolipids at temperatures >19 ºC in the northern Adriatic Sea, particularly from cyanobacterial synthesis of MGs. The sensitivity of photoautotrophs to thermal stress was also explored by Yang et al. (2006), who showed that DGs and MGs both increase the thermal stability of photosystem II, while phospholipids significantly decrease it. Experiments with a wild-type and mutant *Chlamydomonas reinhardtii* have shown that SQs are an essential component of thylakoid membranes to maintain stability under heat stress (Sato et al., 2003), although at considerably more extreme temperatures (41 ºC). Heat stress has also been linked to the production of TAGs (Elsayed et al., 2017; Fakhry and El Maghraby, 2015), which can draw acyl units from degraded membrane lipids (Holm et al., 2022).

Interestingly, the relative abundance of DGs in our experiment shows the most prominent (R^2 of 0.35-0.44), and statistically significant ($p < 0.05$), linear relationship with temperature (see Fig. S3A). While temperature was not identified as an important variable to the prediction of DGs in either decision tree analysis, this may be due to other covariates, such as pH and O_2, masking the effect of temperature. Our results indicate that phytoplankton may either produce DGs in greater abundance to alleviate thermal instability in photosystem II, or preferentially degrade other thylakoid membranes (i.e., PGs, SQs, or MGs) in response to heat stress, leaving the remaining IPL pool relatively enriched in DGs. While several individual MG and SQ molecules did demonstrate linear responses to temperature (Fig. 3), other stressors such as N availability, pH, and light levels may confound the effects of temperature in the overall abundance of these lipid classes.

Deleted: experiment

Deleted:

Deleted:

Deleted:

Deleted: ¶

Deleted: This is likely due to the narrow temperature range observed during the experiment (17.3 - 21.6 ºC), which mirrors the natural variability observed in Callao (average monthly ranges ~16.6-19.6 ºC from 2017 to 2019(Masuda et al., 2023).…

Deleted: c

Deleted: ould

Formatted: Highlight

Formatted: Highlight

Formatted: Highlight

Formatted: Highlight

Deleted: Additional detailed analyses of core fatty acids associated with changing temperatures may elucidate the sources of acyl units for TAG production under heat stress.

4.2.5 Light Availability

Bach et al. (2020) considered the overall productivity in these mesocosm experiments to be co-limited by N and light availability, which have been identified as key limiting factors in eastern boundary upwelling systems (Messié and Chavez, 2015). In our experiment, initial high biomass productivity led to self-shading effects that significantly reduced the PAR (Bach et al., 2020). While the maximum photon flux densities measured at noon over the course of the experiment were ~500 – 600 µmol $m^{-2}s^{-1}$, only ~5-22% and < 4% were measured in surface (~2 m) and subsurface (17 m) waters, respectively, from all four mesocosms. While both depth-integrated samples in our experiment are likely from light-limited planktonic communities, most PAR values (> 15% i.e., 75-132 µmol $m^{-2}s^{-1}$) in surface waters still demonstrate sufficiently high levels that can affect lipid production and accumulation (Gonçalves et al., 2013), especially under the combined effects of N-deprivation (Yeesang and Cheirsilp, 2011; Jiang et al., 2011).

Light levels are identified by the Random Forest analyses to be a significant variable in the prediction of MGs, SQs, PGs, and PCs (Figs. 4, 6, and 7). While few studies have explored the direct effects of irradiance levels on IPL headgroup distributions, experimental cultures of *Tichocarpus crinitus* found increased IPL production of SQs, PGs, and PCs amongst shade-grown algae (Khotimchenko and Yakovleva, 2005). In *Tichocarpus crinitus* cultures, MGs, one of the most abundant thylakoid lipids, show decreased abundances under low light conditions (Khotimchenko and Yakovleva, 2005). Our results show that both MGs and SQs are present in greater relative and absolute abundances in the surface waters where light is less limited or potentially inhibitive at times, suggesting an impact on thylakoid lipid compositions to maintain efficient photosynthetic rates under changing light conditions. MGs have been shown to provide important photoprotective and antioxidant mechanisms in diatoms (Wilhelm et al., 2014), potentially explaining their higher abundance in the surface waters and the significance of light in the Random Forest models. While the exact function of SQs in thylakoid membranes remains unclear, they have been observed to act as an antagonist to the aggregating action of MGs (Goss et al., 2009), leading to a disaggregating effect on light harvesting complexes (Wilhelm et al., 2014). The latter potentially reflects planktonic responses to variable PAR (5-22%) in the surface via adjustment of the proportions of SQs and MGs in the thylakoids (Gabruk et al., 2017; Nakajima et al., 2018).

The PC lipid class, primarily found in extrachloroplast membranes (Mimouni et al., 2018), consistently exhibits greater relative abundance in the subsurface compared to surface waters. We suggest that light levels at depth may play a role (albeit a secondary one, see Fig. S3B) in non-chloroplast IPL production when algal cells are configured for rapid growth/reproduction. Conversely, under higher light as well as under the combined effects of DIC and N limitation at the surface, algal cells are more prone to survival responses such as TAG production at the expense of IPLs. PG can be found in extrachloroplast membranes but is also an essential component of photosystems I and II, with important roles in electron transport processes (Sakurai et al., 2003; Wada and Murata, 2009; Kobayashi et al., 2017). The overall abundance of PGs contributing to the total

Deleted:

Formatted: Not Highlight

Deleted: dramatically

Deleted: ; Yeesang and Cheirsilp, 2011; Jiang et al., 2011),

Deleted:

Deleted: (and decreased production of MGs)

Deleted: , with greater TAG production under high light intensity (Khotimchenko and Yakovleva, 2004; Hu et al., 2008)

Deleted: TAG production under higher light intensity may serve as a mechanism to prevent photochemical damage of algal cells (Roessler, 1990). Over-production of reactive oxygen species under stress may also cause photoinhibition and damage to membrane lipids, amongst other macromolecules (Hu et al., 2008). The low yield of structural lipids relative to chl-a concentrations in surface waters (Fig. S5) could potentially signal TAG accumulation as active algal growth generally favors the production of structural components (Mock and Gradinger, 2000).

Deleted: ¶

Deleted: , which is

Deleted: likely

IPL pool may be influenced by varying production of certain non-chloroplast membranes under lower light conditions, and other thylakoid membranes under high light conditions, thus possibly explaining the highly variable overall contribution of PGs to the IPL pool. Additional analyses of specific fatty acid structures from intact PGs may illuminate sources within the cell, i.e., thylakoid PGs and extrachloroplastic PGs.

Light intensity has also been shown to have contradictory impacts on fatty acid composition, with some analyses observing increased unsaturation under high light intensity (Liu et al., 2012; Pal et al., 2011). Others observed that excess light energy induces synthesis of saturated (SFAs) or monounsaturated (MUFAs) fatty acids in several algal species to prevent photochemical damage, or the synthesis of polyunsaturated fatty acids (PUFA) for the maintenance of photosynthetic membranes under low light conditions (Khoeyi et al., 2012, Fabregas et al., 2004, Sukenik et al., 1993; Orcutt and Patterson, 1974). However, we see limited evidence in this experiment of a direct correlation between light intensities and fatty acid composition in the multiple linear regressions (Fig. 3). This may be related to differences in optimal irradiance levels between algal groups overlapping to confound any clear patterns.

Given that the normalized PAR in surface waters remains <25%, and that light appears as a variable of significant but secondary importance in the random forest models, our results suggest that under these experimental conditions, low or variable light availability may amplify the effects of other environmental stressors (i.e., nitrogen availability, oxygen concentration, temperature, and inorganic carbon availability). The effects of self-shading from high biomass production early in the experiment, when greater nutrient availability was high, likely contributed to the markedly different IPL distributions observed between surface and subsurface waters. As a result, the fluctuations in PAR may play a role in the observed variations in the relative proportions of prevalent thylakoid membrane IPLs, including MGs, SQs, and PGs.

4.3 Implications of IPL Remodeling in Phytoplankton Membranes

We expect the ongoing changing conditions in the ETSP, such as rising temperatures, ocean acidification, expanding ODZs, and shifts in upwelling-driven nutrient supply, to instigate multiple physiological responses amongst phytoplankton communities. IPL remodeling and the reallocation of resources among algae are likely to have cascading effects on the composition of phytoplanktonic communities, the nutritional value of algal biomass to higher trophic levels, and the cycling of organic carbon and nitrogen in the upper ocean. Here, we explore the potential consequences of these physiological responses to environmental conditions and outline future areas of investigation to better constrain the impacts of IPL remodeling on marine biogeochemistry.

Deleted: Notably in *Tichocarpus crinitus* cultures, MGs, one of the most abundant thylakoid lipids, shows increased abundances under high light (Khotimchenko and Yakovleva, 2005). Our results show both MGs and SQs in greater relative and absolute abundances in the surface samples where light is less limited or potentially inhibitive at times, suggesting a significance in thylakoid lipid compositions to maintain efficient photosynthetic rates under changing light conditions. MGs have been shown to carry out important photoprotective and antioxidant mechanisms in diatoms (Wilhelm et al., 2014), potentially explaining their higher abundance at the surface and the significance of light in the Random Forest models. While the exact function of SQs in thylakoid membranes remains unclear, it has been observed to act as an antagonist to the aggregating action of MGs (Goss et al., 2009), with a disaggregating effect on light harvesting complexes (Wilhelm et al., 2014). The latter potentially reflects planktonic responses to the variable PAR (5-22%) in the surface via adjustment of the proportions of SQs and MGs in the thylakoids

Deleted: .

Deleted: ¶

Deleted: PG can be found in extrachloroplast membranes but is also an essential component of photosystems I and II, with important roles in electron transport processes (S ... [30]

Deleted: Its abundance over time is also one of the most variable at both sampling depths (Fig. 2D).

Deleted:

Deleted: The effect of light on PGs concentration is inconsistent, with no clear pattern emerging between ... [31]

Deleted: The overall abundance of PGs contributing to the total IPL pool may be affected by varying production ... [32]

Deleted: ¶

Deleted: ¶

Deleted: , h

Deleted: .

Deleted: W

Deleted: ttle

Deleted: impact

Deleted: of

Deleted: on

Deleted: , except for several PG moieties with 2 or more unsaturation showing a positive relationship with ligh ... [33]

Deleted: DIC concentration

Deleted: We suggest that the combined stressors may result in TAG synthesis at the expense of IPL production, o ... [34]

4.3.1 Relative adaptability of Phytoplankton Classes to environmental change

IPL classes are either partitioned to the thylakoid membranes (i.e., MG, DG, SQ, and PG) in variable distributions to maintain photosynthetic function, or to extraplastidic membranes under growth/reproductive phases (BL, PC, PE, and PG). As environmental conditions change, the ability of phytoplankton to adjust these IPL compositions may be an important driver controlling the phytoplankton community structure. Within a few days of the ODZ water addition, the mesocosms became oligotrophic, which coincided with a major shift in phytoplankton groups, from predominantly diatoms, Chlorophyceae, and Cryptophyceae to a dominance of 'survivalist' mixotrophic dinoflagellates. An obvious advantage of mixotrophic dinoflagellates to the largely N-limited conditions of this experiment is their ability to extract N from the DON pool, and a lower dependence on light compared to the other previously mentioned phytoplankton groups.

Deleted: scavenge

Deleted: P

To contextualize the impacts of IPL remodeling on the phytoplanktonic community, we performed an additional random forest analysis to identify the most important IPLs (both individual moieties and polar head group totals) in the prediction of individual phytoplankton classes. We applied this analysis to identify what IPL remodeling processes may be more readily available to each major phytoplankton class in this experiment (Fig. 8). While all the phytoplankton classes are likely to produce each IPL class to varying extents, the differences in their relative distributions may provide insight into differences in phytoplankton adaptability under changing environmental conditions. Dinoflagellates are heavily associated with high abundances of the glycolipids SQ and DG, with far less apparent dependence on phospholipids and MGs (Fig. 8). The dominance of dinoflagellate biomass is attributed to the severe scarcity of inorganic nitrogen and relatively low light intensity due to self-shading effects (Bach et al., 2020). Dinoflagellates may also take advantage of the recycling of N-bearing PCs and BLs to alleviate nitrogen limitation or to produce energy storing TAGs. The high proportion of DGs and SQs and recycling of MGs may also prove advantageous under high pH/low pCO_2 conditions in surface waters, alleviating pH stressors, or the energy investment in active HCO_3^- transport for photosynthesis. These IPL remodeling strategies may have played a role in the dominance of dinoflagellates under the post-upwelling experimental conditions.

In the early phases of the experiment and when inorganic N is readily available, diatoms (and to a lesser extent Cryptophyceae and Chlorophyceae) dominate the water column biomass. Each of these phytoplankton classes (as well as *Synechococcus*) indicates a greater dependence of the N-bearing PCs and/or BLs, potentially signaling a reduced capacity to scavenge these extrachloroplastic IPLs within the cell for N, or as substrates for TAG production. Notably, these phytoplankton consistently make up a greater proportion of the total chl-a pool in subsurface waters, suggesting an ability to accommodate the lower O_2 concentrations and pH in exchange for greater N availability (see summary in Fig. 8). Some of this adaptability may be related to the recycling of MGs for additional acyl units under hypoxia (most likely amongst Chlorophyceae and *Synechococcus*), and/or the generally higher relative production of structural membrane lipids under low light growth conditions (see impact of light discussion above).

In the Eastern Tropical South Pacific (ETSP), upwelling events exhibit a distinctive trend of increasing frequency and intensity, setting it apart from other eastern boundary systems (Abrahams et al., 2021; Oyarzún and Brierley, 2019). This phenomenon brings about important changes in environmental conditions, including a decrease in sea surface temperature (~0.37°C, average from 1982 to 2019, Abrahams et al., 2021) alongside oxygen reduction and reduced pH in the coastal zones of the region (Pitcher et al., 2021). Simultaneously, there is an observed boost in primary productivity (Gutierrez et al., 2011; Tretkoff, 2011). The impact of strong upwelling, followed by rapid thermal stratification when upwelling subsides, could signify abrupt changes that affect the community structure of phytoplankton (Gutierrez et al., 2011). Such environmental changes favor species better adapted to stress conditions, such as mixotrophic dinoflagellates and silicoflagellates, at the expense of diatom populations (Hallegraeff, 2010), which could translate to a decrease in highly nutritious saturated fatty acids for higher trophic levels (Hauss et al., 2012). Furthermore, a potential reduction in diatom biomass and diversity could have consequences on the ocean biological carbon pump (Tréguer et al., 2018).

Deleted: . A reduction in diatom biomass

Deleted: s

Under the ongoing and projected scenarios of climate change, our mesocosm experiment demonstrates how shifts in the phytoplankton community translate into changes in the lipid composition of their cell membranes. This adds weight to the school of thought that lipid remodeling amongst the phytoplankton community could have repercussions at higher trophic levels, as recently discussed by Holm et al. (2022), and on ocean biogeochemistry as we discuss below.

4.3.2 Cycling of Carbon, Nitrogen, and Sulfur

Combined, neutral (TAGs) and polar lipids (IPLs) make up on the order of 17.6% to 34.7% of the cell by dry weight under N-replete and N-deprived conditions, respectively (Morales et al., 2021), with other environmental stressors able to compound the accumulation of neutral lipids (Zienkiewicz et al., 2016). This represents a considerable portion of algal cellular carbon, and total water column carbon stocks that supply the transfer of fatty acids to higher trophic levels (Twining et al., 2020). Trophic transfer of fatty acids to grazing zooplankton may be affected by the relative contribution of polar and neutral lipids, as they can have significantly different turnover rates (Burian et al., 2020). This suggests that the relative concentrations of TAGs/IPLs in phytoplanktonic communities may impact the rates of fatty acid remineralization or uptake into higher trophic levels. Additionally, while our analysis did not focus on individual fatty acid structures, other experiments investigating the effects of increasing pCO_2 and nitrogen deficiency have demonstrated a reduction in the relative production of essential fatty acids resulting in negative reproductive effects on primary consumers (Meyers et al., 2019). In this context, our IPL results reveal modifications (among polar head groups, carbon numbers, and unsaturations) in response to divergent environmental conditions. However, further investigation of the relative concentrations and turnover rates between TAGs and IPLs, in addition to the production of essential fatty acids, are critical next steps in assessing the impacts of IPL remodeling on trophic transfer processes.

While IPLs are not a major source of cellular N compared to proteins, the highly labile nature of these molecules after cell death may be a potential source of rapidly recycled N via bacterial hydrolysis. On average, N-bearing IPLs such as PCs or BLs, consist of ~2% N by molecular weight (estimated based on a typical 700g/mol betaine lipid). Based on their abundance, they could contribute as much as 10.7 nmol/L of inorganic N in the highly N depleted surface waters of this experiment. Inorganic N species are exceedingly low, and often below the limit of detection (< ~0.1 µmol/L, see methods for details), particularly in the surface samples for most of the experiment after the OMZ water addition. Thus, it is possible that the rapid degradation and recycling of N from IPLs could prove to be an additional supply of N under extremely limiting conditions. Given the diel variability in TAG production via eukaryotic phytoplankton and the potential impacts on energy and carbon fluxes (Becker et al., 2018), further analysis is needed to determine at what temporal scale IPLs may be recycled for TAG synthesis. While Becker et al. (2018) did not find evidence of diacylglycerol transferase (DGAT) activity related to diel cycles, additional investigations of other transferases or lipases relevant to the degradation of IPLs (e.g., PDAT or PGD) are critical.

IPLs may also be an important intermediate in the surface ocean sulfur cycle. Sulfur metabolites produced by phytoplankton (Durham et al., 2019) play central roles in microbial food webs by functioning in metabolism, contributing to membrane structure, supporting osmotic and redox balance, and acting as allelochemicals and signaling molecules (Moran and Durham, 2019). SQs are highly abundant IPLs, particularly in surface waters, and can constitute up to 60 nmol S/L, potentially contributing to a significant proportion of the dissolved organic S in this region (ranging from ~100-225 nmol/L; Lennartz et al., 2019). The ability to catabolize SQs is widespread in heterotrophic bacteria and provides a highly ubiquitous source of sulfur (and carbon) substrates in the synthesis of other essential sulfur metabolites (Speciale et al., 2016). As such, SQs are considered major contributors to the global biosulfur cycle (Goddard-Borger and Williams, 2017) and their considerable production in phytoplankton membranes may be augmented by changes in temperature, light availability (i.e., shading effects), and pH (see discussion above).

Lipids are also sources of dissolved organic carbon (DOC) following hydrolysis by bacterial extracellular enzymes (Myklestad, 2000). Lipids have been observed as the most highly aged component of DOC and are considerably longer lived than lipids found in suspended POC (Loh et al., 2004). However, much of the DOC pool remains uncharacterized (Nebbioso and Piccolo, 2013; Hansell and Carlson, 2014) and little is known regarding the specific processes forming refractory DOC fractions (Hansell, 2013). Yet, preliminary estimates of the total production of relatively refractory DOC (>100-year lifetime) suggest potential significance to global biogeochemistry (Legendre et al., 2015). Furthermore, it is yet unclear as to how DOC cycling may be affected by changing ocean conditions (Wagner et al., 2020). Understanding the degradation pathways involved with abundant lipid pools and how they may contribute to the DOC pool in the surface ocean is of crucial importance to constraining the fluxes of refractory organic carbon pools.

Deleted: TAGs and IPLs

Deleted: Lipids

Deleted: are also sources of dissolved organic carbon (DOC)

Deleted: via

Deleted: following

Deleted: hydrolysis by bacterial extracellular enzymes (Myklestad, 2000). Lipids have been observed as the most highly aged component of DOC and are considerably longer lived than lipids found in suspended POC (Loh et al., 2004). However, much of the DOC pool remains uncharacterized (Nebbioso and Piccolo, 2013; Hansell and Carlson, 2014) and little is known regarding the specific processes forming refractory DOC fractions (Hansell, 2013).

Deleted: Yet, preliminary estimates of the total production of relatively refractory DOC (>100-year lifetime) suggest potential significance to global biogeochemistry (Legendre et al., 2015).

Deleted: Furthermore, it is yet unclear as to how DOC cycling may be affected by changing ocean conditions (Wagner et al., 2020).

Deleted: Yet, preliminary estimates of the total production of relatively refractory DOC (>100-year lifetime) suggest potential significance to global biogeochemistry (Legendre et al., 2015).

Deleted: Understanding the degradation pathways involved with abundant lipid pools and how they may contribute to the DOC pool in the surface ocean is of crucial importance to constraining the fluxes of refractory organic carbon pools.

Deleted: ¶

Deleted: ¶

Deleted: remodeling for the purposes of TAG production

5 Conclusions

We investigated the potential for phytoplankton to evoke lipid remodeling in response to multiple environmental stressors during a two-month mesocosm experiment in the Eastern Tropical South Pacific Ocean off the coast of Peru. Our study is motivated by the need of understanding how the expected changes in oceanographic conditions due to climate in this area will impact the phytoplanktonic communities driving primary productivity in the surface ocean, the chemistry of their cell membranes, and thus the chemical composition of particulate organic matter. A key aspect of our efforts was to statistically separate the relative roles of phytoplankton community composition and lipid remodeling in response to multiple environmental stressors on the composition of the environmental algal lipidome over time. By using a combination of multiple linear regressions, classification and regression trees, and random forest analyses, we report evidence of multiple environmental variables potentially imparting controls on IPL head groups, many of which are known to have specific functions in the chloroplast. The main takeaways of our study include:

- IPLs are effective predictors of changes in the prevailing sources of phytoplankton biomass throughout the experiment.
- The proportion of glycolipids (MG and SQ) increases at higher temperatures, possibly to maintain thermal stability of the photosynthetic apparatus in response to thermal stress.
- The relationship between light levels and the distribution of MGs and PGs possibly invokes photoprotective and antioxidant mechanisms provided by MGs, as well as the role of PGs in electron transport processes in photosystems I and II.
- Differences in the abundance of glycolipids between surface and subsurface waters appear to covary with oxygen availability. We expect this difference to be driven by the degradation of MGs and DGs under anaerobiosis or oxygen stress.
- The reduction in N-bearing IPLs (i.e. BLs and PE) and the higher abundance of non-N-bearing IPLs (i.e., PG, SQ and MG) under more N-limited conditions suggests a possible IPL substitution mechanism to compensate for N limitation.
- Whereas our study does not include the analysis of TAGs, our results are consistent with broader work suggesting that IPLs may be used as a substrate for the generation of acyl chains in TAG production in response to environmental stressors such as N limitation, variable pH or inorganic carbon availability, hypoxia, and varying light levels. However, such mechanism in this mesocosm experiment remains to be tested in future work.
- The cellular adaptations listed above likely contribute to the observed shifts in cellular content from structural or extrachloroplastic membrane lipids (i.e., PCs, PEs, BLs, and certain PGs) under high growth conditions, to thylakoid/plastid membrane lipids (i.e., MGs, DGs, SQs, and certain PGs) while exposed to environmental stressors.

We hypothesize that these remodeling processes may involve major shifts in the elemental stoichiometry of the cell, and thus alter the fluxes of C, N, and S to higher trophic levels, signaling potential impacts on the broader cycling of these biorelevant elements under different scenarios of future environmental change. Therefore, we suggest that future studies addressing the

Deleted: Changing oceanographic conditions in the E ... [35]
Deleted: Furthermore,
Deleted: ing
Deleted: change are expected to result in shifts within
Deleted: that
Deleted: e
Deleted: .
Deleted:
Deleted: Thus it remains essential to determine how ... [36]
Deleted: as reflected in the membrane lipid pool
Deleted: W
Deleted: Temperature significantly impacts various c ... [37]
Deleted: se relationships
Deleted:
Deleted: the production ofIPLs are good predictors ... [39]
Deleted: , particularly SQ, DG, and PE for dinoflag ... [40]
Deleted: *Synechococcus.*
Formatted ... [41]
Formatted ... [38]
Deleted: greater
Deleted: s
Deleted: found
Formatted ... [42]
Deleted: We also observed
Deleted: s
Deleted: ,
Deleted: ing
Deleted: ,
Deleted: the
Deleted: at times
Deleted: highlighting
Deleted: a
Deleted: nd
Deleted: ,
Deleted:
Deleted: possibly regulated by light availability
Formatted ... [43]
Deleted: Furthermore, t
Deleted: variations in the
Deleted: such as MG, DG, and SQ
Deleted: between
Deleted: different groups
Deleted: of
Deleted: among
Deleted: phytoplankton at the
Deleted: compared
Deleted: to the
Deleted: be
Deleted: regulated by
Deleted: and may
Formatted ... [44]

biogeochemical consequences of climate change in the Eastern Tropical South Pacific Ocean must include the role of lipid remodeling in phytoplankton.

Data availability

The environmental study data are available at: https://doi.org/10.1594/PANGAEA.923395 (Bach et al., 2020). Biomarkers metadata that generates and supports the findings of this study and R code are available in: https://github.com/Guachan/IPLs-KOSMOS/tree/0.1.0 (https://doi.org/10.5281/zenodo.10408453, Cantarero, 2023).

Author contribution

JS and SC designed the study. JS funded the study. JS and CV funded sample collection during the mesocosm experiment. UL and LTB designed, funded, organized, and carried out the mesocosm experiment. PA, JS, LTB, and UR carried out sample collection. SIC led laboratory and analytical work with the assistance of ND and under the supervision of JS. SEI carried out data analysis. SIC, JET, BCS, and BR performed statistical analyzes. SIC wrote the manuscript with major editorial contributions from EF, HA, and JS and with comments from all co-authors.

Deleted: SIC wrote the manuscript with comments from all co-authors

Competing interests

The authors declare that they have no conflict of interest. At least one of the (co-)authors is a member of the editorial board of Biogeosciences.

Acknowledgments

We extend our gratitude to all participants in the KOSMOS Peru 2017 study for their invaluable assistance in mesocosm sampling and maintenance. Our special thanks go to the dedicated staffs from GEOMAR-Kiel and IMARPE for their support throughout the planning, preparation, and execution of this study. We are particularly grateful to A. Ludwig, M. Graco, D. Gutierrez, A. Paul, S. Feiersinger, K. Schulz, J.P. Bednar, P. Fritsche, P. Stange, A. Schukat, and M. Krudewig. We also express our appreciation to the captains and crews of BAP Morales, IMARPE VI, and BIC Humboldt for their support during the deployment and recovery of the mesocosms. We extend special thanks to the Marina de Guerra del Perú, specifically the submarine section of the navy in Callao, the Dirección General de Capitanías y Guardacostas, and the Club Náutico Del Centro Naval. The KOSMOS Peru 2017 took place within the framework of the cooperation agreement between IMARPE and GEOMAR through the German Federal Ministry of Education and Research (BMBF) project ASLAEL 12-016 and the national project Integrated Study of the Upwelling System off Peru developed by the Directorate of Oceanography and Climate Change of IMARPE, PPR 137 CONCYTEC. We acknowledge all members of the Organic Geochemistry Laboratory in addition to K. Rempfert, S. Kopf. T. Marchitto, N. Lovenduski at the University of Colorado Boulder, and M. Long at NCAR, for fruitful discussions.

Financial support

This study was funded by the US National Science Foundation CAREER Award 2047057 "MIcrobial Lipidomics in Changing Oceans" (MILCO) to J. Sepúlveda. S. Cantarero and J. Sepúlveda acknowledge additional support from the Department of Geological Sciences and the Center for the Study of Origins at the University of Colorado Boulder. We thank the Millennium Institute of Oceanography (IMO) ICN12_019 through the Agencia Nacional de Investigación y Desarrollo (ANID)—Millennium Science Initiative Program—for providing funding for sample collection. The KOSMOS Peru 2017 was funded by the Collaborative Research Centre SFB 754 Climate-Biogeochemistry Interactions in the Tropical Ocean, funded by the German Research Foundation (DFG) to U. Riebesell. Additional funding was provided by the EU project AQUACOSM

Deleted:

through the European Union's Horizon 2020 research and innovation program under grant agreement no. 731065 and through the Leibniz Award 2012, granted to Ulf Riebesell.

References

Abida, H., Dolch, L.J., Meï, C., Villanova, V., Conte, M., Block, M.A., Finazzi, G., Bastien, O., Tirichine, L., Bowler, C., Rébeillé, F., Petroutsos, D., Jouhet, J., Maréchal, E.: Membrane glycerolipid remodeling triggered by nitrogen and phosphorus starvation in Phaeodactylum tricornutum. Plant Physiology, 167, 118–136, , https://doi.org/10.1104/pp.114.252395, 2015. Abrahams, A., Schlegel, R. W., and Smit, A. J.: Variation and change of upwelling dynamics detected in the world's eastern boundary upwelling systems, Front. Mar. Sci., 8, 626411, doi: 10.3389/fmars.2021.626411, 2021.

Arístegui, J. and Harrison, W. G.: Decoupling of primary production and community respiration in the ocean: Implications for regional carbon studies, Aquat. Microb. Ecol., 29(2), 199–209, doi:10.3354/ame029199, 2002.

Arrigo, K. R.: Marine microorganisms and global nutrient cycles, Nature, 437(7057), 349–355, doi:10.1038/nature04159, 2005.

Azov, Y.: Effect of pH on inorganic carbon uptake in algal cultures, Appl. Environ. Microbiol., 43(6), 1300–1306, doi:10.1128/aem.43.6.1300-1306.1982, 1982.

Bach, L. T., Alvarez-Fernandez, S., Hornick, T., Stuhr, A. and Riebesell, U.: Simulated ocean acidification reveals winners and losers in coastal phytoplankton, PLoS One, 12(11), 1–22, doi: 10.1371/journal.pone.0188198, 2017.

Bach, L. T., Paul, A. J., Boxhammer, T., von der Esch, E., Graco, M., Schulz, K. G., Achterberg, E., Aguayo, P., Arístegui, J., Ayón, P., Baños, I., Bernales, A., Boegeholz, A. S., Chavez, F., Chavez, G., Chen, S. M., Doering, K., Filella, A., Fischer, M., Grasse, P., Haunost, M., Hennke, J., Hernández-Hernández, N., Hopwood, M., Igarza, M., Kalter, V., Kittu, L., Kohnert, P., Ledesma, J., Lieberum, C., Lischka, S., Löscher, C., Ludwig, A., Mendoza, U., Meyer, J., Meyer, J., Minutolo, F., Cortes, J. O., Piiparinen, J., Sforna, C., Spilling, K., Sanchez, S., Spisla, C., Sswat, M., Moreira, M. Z. and Riebesell, U.: Factors controlling plankton community production, export flux, and particulate matter stoichiometry in the coastal upwelling system off Peru, Biogeosciences, 17(19), 4831–4852, doi:10.5194/bg-17-4831-2020, 2020.

Bakun, A., Field, D. B., Redondo-Rodriguez, A. and Weeks, S. J.: Greenhouse gas, upwelling-favorable winds, and the future of coastal ocean upwelling ecosystems, Glob. Chang. Biol., 16(4), 1213–1228, doi:10.1111/j.1365-2486.2009.02094.x, 2010.

Barlow, R. G., Cummings, D. G. and Gibb, S. W.: Improved resolution of mono- and divinyl chlorophylls a and b and zeaxanthin and lutein in phytoplankton extracts using reverse phase C-8 HPLC, Mar. Ecol. Prog. Ser., 161, 303–307, http://www.jstor.org/stable/24859034, 1997.

Becker, K.W., Collins, J.R., Durham, B.P., Groussman, R.D., White, A.E., Fredricks, H.F., Ossolinski, J.E., Repeta, D.J., Carini, P., Armbrust, E.V. and Van Mooy, B.A., Daily changes in phytoplankton lipidomes reveal mechanisms of energy storage in the open ocean. Nature communications 9, 5179, https://doi.org/10.1038/s41467-018-07346-z, 2018.

Deleted: Missing but cited in main text: Abida et al 2015 (Intro: L88)

Deleted: ¶

Behrenfeld, M. J., O'Malley, R. T., Siegel, D. A., McClain, C. R., Sarmiento, J. L., Feldman, G. C., Milligan, A. J., Falkowski, P. G., Letelier, R. M. and Boss, E. S.: Climate-driven trends in contemporary ocean productivity, Nature, 444(7120), 752–755, doi:10.1038/nature05317, 2006.

Benjamini, Y., and Yosef Hochberg, Y., Controlling the False Discovery Rate: A Practical and Powerful Approach to Multiple Testing, Journal of the Royal Statistical Society: Series B (Methodological), 57, 289–300, doi:10.1111/j.2517-6161.1995.tb02031.x, 1995.

Berry, J. and Bjorkman, O.: Photosynthetic Response and Adaptation to Temperature in Higher Plants, Annu. Rev. Plant Physiol., 31(1), 491–543, doi:10.1146/annurev.pp.31.060180.002423, 1980.

Brandsma, J.: The origin and fate of intact polar lipids in the marine environment, PhD thesis, Dept. of Marine Organic Biogeochemistry, Royal Netherlands Institute for Sea Research (NIOZ), pp. 224, ISBN: 978-90-6266-286-9, 2011.

Bligh, E. G., and Dyer, W.J.: A rapid method of total lipid extraction and purification, Canadian journal of biochemistry and physiology, 37(8), 911-917, doi:10.1139/o59-099, 1959.

Biau G,, and Scornet E. A random forest guided tour. Test; 25(2): 197–227, https://doi.org/10.1007/s11749-016-0481-7, 2016.

Boulesteix, A. L., Janitza, S., Kruppa, J., & König, I. R.: Overview of random forest methodology and practical guidance with emphasis on computational biology and bioinformatics. Wiley Interdisciplinary Reviews: Data Mining and Knowledge Discovery, 2(6), 493–507, https://doi.org/10.1002/widm.1072, 2012.

Breiman, L., Friedman, J.H., Olshen, R.A., & Stone, C.J.: Classification And Regression Trees (1st ed.)., Chapman and Hall/CRC, https;//doi.org/10.1201/9781315139470, 1984.

Breiman, L.: Random Forests, Mach. Learn., 45, 5–32, https://doi.org/10.1023/A:1010933404324, 2001.

Browning, T. J., Rapp, I., Schlosser, C., Gledhill, M., Achterberg, E. P., Bracher, A. and Le Moigne, F. A. C.: Influence of Iron, Cobalt, and Vitamin B12 Supply on Phytoplankton Growth in the Tropical East Pacific During the 2015 El Niño, Geophys. Res. Lett., 45(12), 6150–6159, doi:10.1029/2018GL077972, 2018.

Bronk, D. A., See, J. H., Bradley, P., & Killberg, L.: DON as a source of bioavailable nitrogen for phytoplankton. Biogeosciences, 4(3), 283–296. https://doi.org/10.5194/bg-4-283-2007, 2007.

Burian, A., Nielsen, J. M., Hansen, T., Bermudez, R. and Winder, M.: The potential of fatty acid isotopes to trace trophic transfer in aquatic food-webs, Philos. Trans. R. Soc. B Biol. Sci., 375(1804), doi:10.1098/rstb.2019.0652, 2020.

Cantarero, S., Henríquez-Castillo, C., Dildar, N., Vargas, C., von Dassow, P., Cornejo-D'Ottone, M. and Sepúlvada, J.: Size-fractionated contribution of microbial biomass to suspended organic matter in the Eastern Tropical South Pacific oxygen minimum zone, Front. Mar. Sci., 7:540643. doi: 10.3389/fmars.2020.540643, 2020.

Capone, D. G. and Hutchins, D. A.: Microbial biogeochemistry of coastal upwelling regimes in a changing ocean, Nat. Geosci., 6(9), 711–717, doi:10.1038/ngeo1916, 2013.

Carter, B. R., Radich, J. A., Doyle, H. L. and Dickson, A. G.: An automated system for spectrophotometric seawater pH measurements, Limnol. Oceanogr. Methods, 11(JAN), 16–27, doi:10.4319/lom.2013.11.16, 2013.

Deleted: Missing: Boulesteix et al 2012 reference: found in CART methods section

Deleted: Missing: Bronk et al 2007 from 4.2.1 nutrient availability…

1975 Chavez, F. P. and Messié, M.: A comparison of Eastern Boundary Upwelling Ecosystems, Prog. Oceanogr., 83(1–4), 80–96,
1976 doi:10.1016/j.pocean.2009.07.032, 2009.
1977 Chen, S., Riebesell, U., Schulz, K. G., Esch, E. Von Der, Achterberg, E. P. and Bach, L. T.: Temporal dynamics of surface
1978 ocean carbonate chemistry in response to natural and simulated upwelling events during the 2017 coastal El Niño near
1979 Callao, Peru., Biogeosciences, 19,295-312, https://doi.org/10.5194/bg-19-295-2022, 2022.
1980 Chen, X., and H. Ishwaran.: Random forests for genomic data analysis. Genomics 99: 323–329,
1981 https://doi.org/10.1016/j.ygeno.2012.04.003, 2012. Coverly, S., Kérouel, R. and Aminot, A.: A re-examination of matrix
1982 effects in the segmented-flow analysis of nutrients in sea and estuarine water, Anal. Chim. Acta, 712, 94–100,
1983 doi:10.1016/j.aca.2011.11.008, 2012.
1984 Dahlqvist, A., Ståhl, U., Lenman, M., Banas, A., Lee, M., Sandager, L., Ronne, H. and Stymne, S.: Phospholipid:diacylglycerol
1985 acyltransferase: An enzyme that catalyzes the acyl-CoA-independent formation of triacylglycerol in yeast and plants,
1986 Proc. Natl. Acad. Sci. U. S. A., 97(12), 6487–6492, doi:10.1073/pnas.120067297, 2000.
1987 Ding, H. and Sun, M. Y.: Biochemical degradation of algal fatty acids in oxic and anoxic sediment-seawater interface systems:
1988 Effects of structural association and relative roles of aerobic and anaerobic bacteria, Mar. Chem., 93(1), 1–19,
1989 doi:10.1016/j.marchem.2004.04.004, 2005.
1990 DiTullio, G. R., Geesey, M. E., Mancher, J. M., Alm, M. B., Riseman, S. F. and Bruland, K. W.: Influence of iron on algal
1991 community composition and physiological status in the Peru upwelling system, Limnol. Oceanogr., 50(6), 1887–1907,
1992 doi:10.4319/lo.2005.50.6.1887, 2005.
1993 Durham, B. P., Boysen, A. K., Carlson, L. T., Groussman, R. D., Heal, K. R., Cain, K. R., Morales, R. L., Coesel, S. N.,
1994 Morris, R. M., Ingalls, A. E. and Armbrust, E. V.: Sulfonate-based networks between eukaryotic phytoplankton and
1995 heterotrophic bacteria in the surface ocean, Nat. Microbiol., 4(10), 1706–1715, doi:10.1038/s41564-019-0507-5, 2019.
1996 Dutkiewicz, S., Ward, B. A., Monteiro, F. and Follows, M. J.: Interconnection of nitrogen fixers and iron in the Pacific Ocean:
1997 Theory and numerical simulations, Global Biogeochem. Cycles, 26(1), 1–16, doi:10.1029/2011GB004039, 2012.
1998 Dutkiewicz, S., Morris, J. J., Follows, M. J., Scott, J., Levitan, O., Dyhrman, S. T. and Berman-Frank, I.: Impact of ocean
1999 acidification on the structure of future phytoplankton communities, Nat. Clim. Chang., 5(11), 1002–1006,
2000 doi:10.1038/nclimate2722, 2015.
2001 Elsayed, K. N. M., Kolesnikova, T. A., Noke, A. and Klöck, G.: Imaging the accumulated intracellular microalgal lipids as a
2002 response to temperature stress, 3 Biotech, 7(1), doi:10.1007/s13205-017-0677-x, 2017.
2003 Missing: Fabregas et al 2004 from 4.2.5 light availability
2004 Fakhry, E. M. and El Maghraby, D. M.: Lipid accumulation in response to nitrogen limitation and variation of temperature in
2005 nannochloropsis salina, Bot. Stud., 56, 6, doi:10.1186/s40529-015-0085-7, 2015.
2006 Fan, J., Andre, C. and Xu, C.: A chloroplast pathway for the de novo biosynthesis of triacylglycerol in Chlamydomonas
2007 reinhardtii, FEBS Lett., 585(12), 1985–1991, doi:10.1016/j.febslet.2011.05.018, 2011.

Deleted: ,

Commented [5]: missing reference from text

Deleted: MISSING: Chen and Ishwaran 2012 from CART methods section

Deleted: ¶

Deleted: Clarke, K. R.: Non-parametric multivariate analyses of changes in community structure, Aust. J. Ecol., 18(1), 117–143, doi:10.1111/j.1442-9993.1993.tb00438.x, 1993.

Deleted: ¶

Deleted: Du, Z.Y., and Christoph Benning, C.: Triacylglycerol accumulation in photosynthetic cells in plants and algae. Lipids in plant and algae development, 179-205, 2016.

Deleted: ¶

Fuenzalida, R., Schneider, W., Garcés-Vargas, J., Bravo, L. and Lange, C.: Vertical and horizontal extension of the oxygen minimum zone in the eastern South Pacific Ocean, Deep. Res. Part II Top. Stud. Oceanogr., 56(16), 992–1003, doi:10.1016/j.dsr2.2008.11.001, 2009.

Gabruk, M., Mysliwa-Kurdziel, B., and Kruk, J.. MGDG, PG and SQDG regulate the activity of light-dependent protochlorophyllide oxidoreductase. Biochem. J. 474, 1307–1320. doi: 10.1042/BCJ20170047, 2017.

Gardner, R. D., Cooksey, K. E., Mus, F., Macur, R., Moll, K., Eustance, E., Carlson, R. P., Gerlach, R., Fields, M. W. and Peyton, B. M.: Use of sodium bicarbonate to stimulate triacylglycerol accumulation in the chlorophyte Scenedesmus sp. and the diatom Phaeodactylum tricornutum, J. Appl. Phycol., 24(5), 1311–1320, doi:10.1007/s10811-011-9782-0, 2012.

Gardner, R., Peters, P., Peyton, B. and Cooksey, K. E.: Medium pH and nitrate concentration effects on accumulation of triacylglycerol in two members of the chlorophyta, J. Appl. Phycol., 23(6), 1005–1016, doi:10.1007/s10811-010-9633-4, 2011.

Gašparović, B., Godrijan, J., Frka, S., Tomažić, I., Penezić, A., Marić, D., Djakovac, T., Ivančić, I., Paliaga, P., Lyons, D., Precali, R. and Tepić, N.: Adaptation of marine plankton to environmental stress by glycolipid accumulation, Mar. Environ. Res., 92, 120–132, doi:10.1016/j.marenvres.2013.09.009, 2013.

Geider, J. R. and Osborne, B. A.: Respiration and microalgal growth: a review of the quantitative relationship between dark respiration and growth, New Phytol., 112(3), 327–341, doi:10.1111/j.1469-8137.1989.tb00321.x, 1989.

Gilly, W. F., Beman, J. M., Litvin, S. Y. and Robison, B. H.: Oceanographic and Biological Effects of Shoaling of the Oxygen Minimum Zone, Ann. Rev. Mar. Sci., 5(1), 393–420, doi:10.1146/annurev-marine-120710-100849, 2013.

Goddard-Borger, and E.D., Williams, S.J., Sulfoquinovose in the biosphere: occurrence, metabolism and functions. Biochem J 1, 474 (5), 827–849, doi: https://doi.org/10.1042/BCJ20160508, 2017.

Gombos, Z. and Murata, N.: Lipids and fatty acids of prochlorothrix hollandica, Plant Cell Physiol., 32(1), 73–77, doi:10.1093/oxfordjournals.pcp.a078054, 1991.

Gonçalves, A. L., Pires, J. C., & Simões, M.: Lipid production of Chlorella vulgaris and Pseudokirchneriella subcapitata. Int. J. Energy Environ. Eng., 4, 14, https://doi.org/10.1186/2251-6832-4-14 2013.

Goss, R., Nerlich, J., Lepetit, B., Schaller, S., Vieler, A. and Wilhelm, C.: The lipid dependence of diadinoxanthin de-epoxidation presents new evidence for a macrodomain organization of the diatom thylakoid membrane, J. Plant Physiol., 166(17), 1839–1854, doi:10.1016/j.jplph.2009.05.017, 2009.

Gu, X., Cao, L., Wu, X., Li, Y., Hu, Q. and Han, D.: A lipid bodies-associated galactosyl hydrolase is involved in triacylglycerol biosynthesis and galactolipid turnover in the unicellular green alga chlamydomonas reinhardtii, Plants, 10(4), doi:10.3390/plants10040675, 2021.

Guckert, J. B., and Cooksey, K.E.: Triglyceride accumulation and fatty acid profile changes in Chlorella (Chlorophyta) during high Ph-induced cell cycle Inhibition, Journal of Phycology, 26, 72-79, https://doi.org/10.1111/j.0022-3646.1990.00072.x, 1990.

Deleted: Franz, J., Krahmann, G., Lavik, G., Grasse, P., Dittmar, T. and Riebesell, U.: Dynamics and stoichiometry of nutrients and phytoplankton in waters influenced by the oxygen minimum zone in the eastern tropical Pacific, Deep. Res. Part I Oceanogr. Res. Pap., 62, 20–31, doi:10.1016/j.dsr.2011.12.004, 2012.

Deleted: ¶

Deleted: Gombos, Z., Várkonyi, Z., Hagio, M., Iwaki, M., Kovács, L., Masamoto, K., Itoh, S. and Wada, H.: Phosphatidylglycerol requirement for the function of electron acceptor plastoquinone QB in the photosystem II reaction center, Biochemistry, 41(11), 3796–3802, doi:10.1021/bi011884h, 2002.

Guschina, I. A., and Harwood, J. L. Algal lipids and their metabolism. In: Borowitzka, M., Moheimani, N. (eds) Algae for Biofuels and Energy. Springer, Dordrecht, pp. 17-36. https://doi.org/10.1007/978-94-007-5479-2_2, 2013.

Gutiérrez, D., Bouloubassi, I., Sifeddine, A., Purca, S., Goubanova, K., Graco, M., Field, D., Méjanelle, L., Velazco, F., Lorre, A., Salvatteci, R., Quispe, D., Vargas, G., Dewitte, B. and Ortlieb, L.: Coastal cooling and increased productivity in the main upwelling zone off Peru since the mid-twentieth century, Geophys. Res. Lett., 38(7), 1–6, doi:10.1029/2010GL046324, 2011.

Hallegraeff, G.M. Ocean climate change, phytoplankton community responses, and harmful algal blooms: a formidable predictive challenge. J. Phycol. 46 (2), 220–235, https://doi.org/10.1111/j.1529-8817.2010.00815.x, 2010.

Hansell, D. A.: Recalcitrant dissolved organic carbon fractions, Ann. Rev. Mar. Sci., 5, 421–445, doi:10.1146/annurev-marine-120710-100757, 2013.

Hansell, D. A., and Carlson, C.A., eds. Biogeochemistry of marine dissolved organic matter. Academic Press, https://doi.org/10.1016/C2012-0-02714-7, 2014.

Harwood, J. L. and Jones, A. L.: Lipid Metabolism in Algae., Advances in Botanical Research, 16, 1-53, https://doi.org/10.1016S0065-2296(08)60238-4, 1989.

Hastie, T., Tibshirani, R. and Friedman, J.: Springer Series in Statistics, Elem. Stat. Learn., 27(2), 83–85, doi:10.1007/b94608, 2009.

Hauss, H., Franz, J., and Sommer, U.: Changes in N:P stoichiometry influence taxonomic composition and nutritional quality of phytoplankton in the Peruvian upwelling, J. Sea Res., 73, 74–85, https://doi.org/10.1016/j.seares.2012.06.010, 2012.

Hemschemeier, A., Casero, D., Liu, B., Benning, C., Pellegrini, M., Happe, T. and Merchant, S. S.: COPPER RESPONSE REGULATOR1-dependent and -independent responses of the Chlamydomonas reinhardtii transcriptome to dark anoxia, Plant Cell, 25(9), 3186–3211, doi:10.1105/tpc.113.115741, 2013.

Henson, S. A., Cael, B. B., Allen, S. R. and Dutkiewicz, S.: Future phytoplankton diversity in a changing climate, Nat. Commun., 12(1), 1–8, doi:10.1038/s41467-021-25699-w, 2021.

Holm, H. C., Fredricks, H. F., Bent, S. M., Lowenstein, D. P., Ossolinski, J. E., Becker, K. W., Johnson, W. M., Schrage, K., & Van Mooy, B. A. S. Global Ocean lipidomes show a universal relationship between temperature and lipid unsaturation. Science, 376, 1487– 1491. https://doi.org/10.1126/science.abn7455, 2022.

Hu, Q., Sommerfeld, M., Jarvis, E., Ghirardi, M., Posewitz, M., Seibert, M. and Darzins, A.: Microalgal triacylglycerols as feedstocks for biofuel production: Perspectives and advances, Plant J., 54(4), 621–639, doi:10.1111/j.1365-313X.2008.03492.x, 2008.

Huertas E., I., Rouco, M., López-Rodas, V. and Costas, E.: Warming will affect phytoplankton differently: Evidence through a mechanistic approach, Proc. R. Soc. B Biol. Sci., 278(1724), 3534–3543, doi:10.1098/rspb.2011.0160, 2011.

Hutchins, D. A., Hare, C. E., Weaver, R. S., Zhang, Y., Firme, G. F., DiTullio, G. R., Alm, M. B., Riseman, S. F., Maucher, J. M., Geesey, M. E., Trick, C. G., Smith, G. J., Rue, E. L., Conn, J. and Bruland, K. W.: Phytoplankton iron limitation

Deleted: Guo, L., Liu, C., Yun, F., Li, Y. and Zhu, Y.: Power coordination control of ±1 100 kV UHVDC system with hierarchical connection mode, Dianli Xitong Zidonghua/Automation Electr. Power Syst., 39(11), 24–30, doi:10.7500/AEPS20140903006, 2015.

Deleted: ¶

in the Humboldt Current and Peru Upwelling, Limnol. Oceanogr., 47(4), 997–1011, doi:10.4319/lo.2002.47.4.0997, 2002.

Hutchins, D. A. and Fu, F.: Microorganisms and ocean global change, Nat. Microbiol., 2(May), doi:10.1038/nmicrobiol.2017.58, 2017.

Irwin, A. J., Finkel, Z. V., Müller-Karger, F. E. and Ghinaglia, L. T.: Phytoplankton adapt to changing ocean environments, Proc. Natl. Acad. Sci. U. S. A., 112(18), 5762–5766, doi:10.1073/pnas.1414752112, 2015.

Jiang, L., Luo, S., Fan, X., Yang, Z. and Guo, R.: Biomass and lipid production of marine microalgae using municipal wastewater and high concentration of CO2, Appl. Energy, 88(10), 3336–3341, doi:10.1016/j.apenergy.2011.03.043, 2011.

Jiang, L. Q., Carter, B. R., Feely, R. A., Lauvset, S. K. and Olsen, A.: Surface ocean pH and buffer capacity: past, present and future, Sci. Rep., 9(1), 1–11, doi:10.1038/s41598-019-55039-4, 2019.

Jin, P., Liang, Z., Lu, H., Pan, J., Li, P., Huang, Q., Guo Y,, Zhong, J., Li, F., Wan, J., Overmans, S., and Xia, J.: Lipid remodeling reveals the adaptations of a marine diatom to ocean acidification. Frontiers in Microbiology, 12, 748445, doi: 10.3389/fmicb.2021.748445, 2021.

Jónasdóttir, S. H.: Fatty acid profiles and production in marine phytoplankton, Mar. Drugs, 17(3), doi:10.3390/md17030151, 2019.

Kato, C., Masui, N., and Horikoshi, K.: Properties of obligately barophilic bacteria isolated from a sample of deep-sea sediment from the Izu-Bonin trench, J. Mar. Biotechnol.., 4, 96-99, https://cir.nii.ac.jp/crid/1573105973909199488, 1996.

Keeling, R. F., Körtzinger, A. and Gruber, N.: Ocean deoxygenation in a warming world, Ann. Rev. Mar. Sci., 2(1), 199–229, doi:10.1146/annurev.marine.010908.163855, 2010.

Kérouel, R. and Aminot, A.: Fluorometric determination of ammonia in sea and estuarine waters by direct segmented flow analysis, Mar. Chem., 57(3–4), 265–275, doi:10.1016/S0304-4203(97)00040-6, 1997.

Khoeyi, Z. A., Seyfabadi, J. and Ramezanpour, Z.: Effect of light intensity and photoperiod on biomass and fatty acid composition of the microalgae, Chlorella vulgaris, Aquac. Int., 20(1), 41–49, doi:10.1007/s10499-011-9440-1, 2012.

Khotimchenko, S. V. and Yakovleva, I. M.: Lipid composition of the red alga Tichocarpus crinitus exposed to different levels of photon irradiance, Phytochemistry, 66(1), 73–79, doi:10.1016/j.phytochem.2004.10.024, 2005.

Khotimchenko, S. V. and Yakovleva, I. M.: Effect of solar irradiance on lipids of the green alga Ulva fenestrata Postels et Ruprecht, Bot. Mar., 47(5), 395–401, doi:10.1515/BOT.2004.050, 2004.

Kobayashi, K., Endo, K. and Wada, H.: Specific distribution of phosphatidylglycerol to photosystem complexes in the thylakoid membrane, Front. Plant Sci., 8(November), 1–7, doi:10.3389/fpls.2017.01991, 2017.

Kong, F., Romero, I. T., Warakanont, J. and Li-Beisson, Y.: Lipid catabolism in microalgae, New Phytol., 218(4), 1340–1348, doi:10.1111/nph.15047, 2018.

Kudela, R. M., Seeyave, S., and Cochlan, W. P.: The role of nutrients in regulation and promotion of harmful algal blooms in upwelling systems, Prog. Oceanogr., 85, 122–135, https://doi.org/10.1016/j.pocean.2010.02.008, 2010.

Deleted: Keeling, R. F. and Garcia, H. E.: The change in oceanic O_2 inventory associated with recent global warming. Proc. Natl. Acad. Sci. U. S. A., 99(12), 7848-7853, https://doi.org/10.1073/pnas.122154899, 2002.

Deleted: ¶

Kumari, P., Bijo, A. J., Mantri, V. A., Reddy, C. R. K. and Jha, B.: Fatty acid profiling of tropical marine macroalgae: An analysis from chemotaxonomic and nutritional perspectives, Phytochemistry, 86, 44–56, doi:10.1016/j.phytochem.2012.10.015, 2013.

Lam, P., Kuypers, M. M. M., Lavik, G., Jensen, M. M., Vossenberg, J. Van De, Schmid, M., Woebken, D., Amann, R., Jetten, M. S. M. and Kuypers, M. M. M.: Revising the nitrogen cycle in the Peruvian oxygen minimum zone Phyllis, Proc. Natl. Acad. Sci., 106(12), 2192–2205, doi:10.1038/nature0415, 2009.

Legendre, L., Rivkin, R. B., Weinbauer, M. G., Guidi, L. and Uitz, J.: The microbial carbon pump concept: Potential biogeochemical significance in the globally changing ocean, Prog. Oceanogr., 134, 432–450, doi:10.1016/j.pocean.2015.01.008, 2015.

Lennartz, S., von Hobe, M., Booge, D., Bittig, H., Fischer, T., Gonçalves-Araujo, R., Ksionzek, K., Koch, B., Bracher, A., Röttgers, R., Quack, B. and Marandino, C.: The influence of dissolved organic matter on the marine production of carbonyl sulfide (OCS) and carbon disulfide (CS_2) in the Eastern Tropical South Pacific, Ocean Sci. Discuss., (March), 1–32, doi:10.5194/os-2019-1, 2019.

Li, X., Benning, C., & Kuo, M. H.: Rapid triacylglycerol turnover in Chlamydomonas reinhardtii requires a lipase with broad substrate specificity. Eukaryotic Cell, 11(12), 1451-1462, doi: 10.1128/EC.00268-12, 2012.

Li-Beisson, Y., Thelen, J. J., Fedosejevs, E. and Harwood, J. L.: The lipid biochemistry of eukaryotic algae, Prog. Lipid Res., 74, 31–68, doi:10.1016/j.plipres2019.01.003, 2019.

Lipp, J. S., Morono, Y., Inagaki, F., and Hinrichs, K.-U.: Significant contribution of Archaea to extant biomass in marine subsurface sediments, Nature, 454, 991–994, https://doi.org/10.1038/nature07174, 2008.

Liu, J., Yuan, C., Hu, G. and Li, F.: Effects of light intensity on the growth and lipid accumulation of microalga Scenedesmus sp. 11-1 under nitrogen limitation, Appl. Biochem. Biotechnol., 166(8), 2127–2137, doi:10.1007/s12010-012-9639-2, 2012.

Liu, B.: Biochemical Characterization of Triacylglycerol Metabolism in Microalgae, PhD thesis, Biochemistry and Molecular Biology, Michigan State University, USA. pp. 165, ISBN: 9781303715174130371517l, 2014.

Loh, A. N., Bauer, J. E. and Druffel, E. R. M.: Variable ageing and storage of dissolved organic components in the open ocean, Nature, 430(7002), 877–881, doi:10.1038/nature02780, 2004.

Luan, J., Zhang, C., Xu, B., Xue, Y., Ren, Y.: The predictive performances of random forest models with limited sample size and different species traits. Fish. Res. 227: 105534, https://doi.org/10.1016/j.fishres.2020.105534, 2020.

Lyon, B. R. and Mock, T.: Polar microalgae: New approaches towards understanding adaptations to an extreme and changing environment, Biology (Basel)., 3(1), 56–80, doi:10.3390/biology3010056, 2014.

Mackey, M. D., Mackey, D. J., Higgins, H. W. and Wright, S. W.: CHEMTAX - A program for estimating class abundances from chemical markers: Application to HPLC measurements of phytoplankton, Mar. Ecol. Prog. Ser., 144(1–3), 265–283, doi:10.3354/meps144265, 1996.

Deleted: Missing: Luan et al 2020: citation present in CART methods section

Deleted: ¶

Masuda, S., Kobayashi, M., Icochea Salas, L.A. and Rosales Quintana, G.M.: Possible link between temperatures in the seashore and open ocean waters of Peru identified by using new seashore water data. Progr. Earth Planet. Sci., 10, 38, https://doi.org/10.1186/s40645-023-00571-1, 2023.

Meador, T. B., Goldenstein, N. I., Gogou, A., Herut, B., Psarra, S., Tsagaraki, T. M. and Hinrichs, K. U.: Planktonic lipidome responses to Aeolian dust input in low-biomass oligotrophic marine mesocosms, Front. Mar. Sci., 4(APR), 1–20, doi:10.3389/fmars.2017.00113, 2017.

Messié, M., Ledesma, J., Kolber, D. D., Michisaki, R. P., Foley, D. G., & Chavez, F. P.: Potential new production estimates in four eastern boundary upwelling ecosystems. Progress in Oceanography, 83(1-4), 151-158, doi: https://doi.org/10.1016/j.pocean.2009.07.018, 2009.

Messié, M. and Chavez, F. P.: Seasonal regulation of primary production in eastern boundary upwelling systems, Prog. Oceanogr., 134, 1–18, doi:10.1016/j.pocean.2014.10.011, 2015.

Meyer, J., Löscher, C. R., Lavik, G. and Riebesell, U.: Mechanisms of P* reduction in the eastern tropical South Pacific, Front. Mar. Sci., 4(JAN), 1–12, doi:10.3389/fmars.2017.00001, 2017.

Meyers, M. T., Cochlan, W. P., Carpenter, E. J. and Kimmerer, W. J.: Effect of ocean acidification on the nutritional quality of marine phytoplankton for copepod reproduction, PLoS One, 14(5), 1–22, doi:10.1371/journal.pone.0217047, 2019.

Mimouni, V., Couzinet-Mossion, A., Ulmann, L., & Wielgosz-Collin, G.. Lipids from microalgae. In: Levine, I. A,, Fleurence,, J. (Eds) Microalgae in health and disease prevention, pp. 109-131, Academic Press, doi: 10.1016/B978-0-12-811405-6.00005-0, 2018.

Min, M.A., Needham, D.M., Sudek, S., Truelove, N.K., Pitz, K.J., Chavez, G.M., Poirier, C., Gardeler, B., von der Esch, E., Ludwig, A., Riebesell, U., Worden, A.Z., Chavez, F.P., 2023. Ecological divergence of a mesocosm in an eastern boundary upwelling system assessed with multi-marker environmental DNA metabarcoding. Biogeosciences 20, 1277–1298. https://doi.org/10.5194/bg-20-1277-2023, 2023.

Moazami-Goudarzi, M. and Colman, B.: Changes in carbon uptake mechanisms in two green marine algae by reduced seawater pH, J. Exp. Mar. Bio. Ecol., 413, 94–99, doi:10.1016/j.jembe.2011.11.017, 2012.

Mock, T. and Gradinger, R.: Changes in photosynthetic carbon allocation in algal assemblages of Arctic sea ice with decreasing nutrient concentrations and irradiance, Mar. Ecol. Prog. Ser., 202, 1–11, doi:10.3354/meps202001, 2000.

Morales, M., Aflalo, C. and Bernard, O.: Microalgal lipids: A review of lipids potential and quantification for 95 phytoplankton species, Biomass and Bioenergy, 150(April), 106108, doi:10.1016/j.biombioe.2021.106108, 2021.

Morán, X. A. G., López-Urrutia, Á., Calvo-Díaz, A. and LI, W. K. W.: Increasing importance of small phytoplankton in a warmer ocean, Glob. Chang. Biol., 16(3), 1137–1144, doi:10.1111/j.1365-2486.2009.01960.x, 2010.

Moran, M. A. and Durham, B. P.: Sulfur metabolites in the pelagic ocean, Nat. Rev. Microbiol., 17(11), 665–678, doi:10.1038/s41579-019-0250-1, 2019.

Morris, A. W. and Riley, J. P.: The determination of nitrate in sea water, Anal. Chim. Acta, 29(C), 272–279, doi:10.1016/S0003-2670(00)88614-6, 1963.

Deleted: MISSING - Messié et al 2009: intro L65

Mullin, J. B. and Riley, J. P.: The colorimetric determination of silicate with special reference to sea and natural waters, Anal. Chim. Acta, 12(C), 162–176, doi:10.1016/S0003-2670(00)87825-3, 1955.

Murphy, J. and Riley, J. P.: A modified single solution method for the determination of phosphate in natural waters, Anal. Chim. Acta, 27(C), 31–36, doi:10.1016/S0003-2670(00)88444-5, 1962.

Myklestad, S. M.: Dissolved Organic Carbon from Phytoplankton, In Wangersky, P. J., (Eds) Marine Chemistry. The Handbook of Environmental Chemistry, Springer, Berlin, Heidelberg, 111–148, doi:10.1007/10683826_5, 2000.

Nakajima, Y., Umena, Y., Nagao, R., Endo, K., Kobayashi, K., Akita, F., Suga, M., Wada, H., Noguchi, T., and Shen, J. R., Thylakoid membrane lipid sulfoquinovosyl-diacylglycerol (SQDG) is required for full functioning photosystem II in Thermosynechococccus elongatus, J. Biol. Chem., 293, 14786-14797, https://doi.org/10.1074/jbc.RA118.004304d, 2018.

Naqvi, S. W. A., Bange, H., Farias, L., Monteiro, P., Scranton, M., & Zhang, J.: Marine hypoxia/anoxia as a source of CH_4 and N_2O. Biogeosciences, 7, https://doi.org/10.5194/bg-7-2159, 2010.Nebbioso, A. and Piccolo, A.: Molecular characterization of dissolved organic matter (DOM): A critical review, Anal. Bioanal. Chem., 405(1), 109–124, doi:10.1007/s00216-012-6363-2, 2013.

Neidleman, S. L.: Effects of temperature on lipid unsaturation, Biotechnol. Genet. Eng. Rev., 5(1), 245–268, doi:10.1080/02648725.1987.10647839, 1987.

Orcutt, D. M. and Patterson, G. W.: Effect of light intensity upon lipid composition of Nitzschia closterium (Cylindrotheca fusiformis), Lipids, 9(12), 1000–1003, doi:10.1007/BF02533825, 1974.

Oyarzún, D. and Brierley, C. M.: The future of coastal upwelling in the Humboldt current from model projections, Clim. Dynam., 52, 599–615, https://doi.org/10.1007/s00382-018-4158-7, 2019.

Pal, D., Khozin-Goldberg, I., Cohen, Z. and Boussiba, S.: The effect of light, salinity, and nitrogen availability on lipid production by Nannochloropsis sp., Appl. Microbiol. Biotechnol., 90(4), 1429–1441, doi:10.1007/s00253-011-3170-1, 2011.

Paul, A. J., Bach, L. T., Schulz, K. G., Boxhammer, T., Czerny, J., Achterberg, E. P., Hellemann, D., Trense, Y., Nausch, M., Sswat, M. and Riebesell, U.: Effect of elevated CO2 on organic matter pools and fluxes in a summer Baltic Sea plankton community, Biogeosciences, 12(20), 6181–6203, doi:10.5194/bg-12-6181-2015, 2015.

Peng, X., Liu, S., Zhang, W., Zhao, Y., Chen, L., Wang, H. and Liu, T.: Triacylglycerol accumulation of Phaeodactylum tricornutum with different supply of inorganic carbon, J. Appl. Phycol., 26(1), 131–139, doi:10.1007/s10811-013-0075-7, 2014.

Pitcher, G. C., Aguirre-Velarde, A., Breitburg, D., Cardich, J., Carstensen, J., Conley, D. J., Dewitte, B., Engel, A., EspinozaMorriberón, D., Flores, G., Garçon, V., Graco, M., Grégoire, M., Gutiérrez, D., Hernandez-Ayon, J. M., Huang, H.-H. M., Isensee, K., Jacinto, M. E., Levin, L., Lorenzo, A., Machu, E., Merma, L., Montes, I., Swa, N., Paulmier, A., Roman, M., Rose, K., Hood, R., Rabalais, N. N., Salvanes, A. G. V., Salvatteci, R., Sánchez, S., Sifeddine, A., Tall, A.

Deleted: Missing: Naqvi et al. 2010 from section 4.2.3 Oxygen

Formatted: Subscript

Deleted: ¶

Formatted: Subscript

Deleted: Pearson, A.: 12.11 Lipidomics for Geochemistry, Treatise Geochem., 12, 2013.

Deleted: ¶

Deleted: Peng, X., Liu, S., Zhang, W., Zhao, Y., Chen, L., Wang, H., & Liu, T.: Triacylglycerol accumulation of Phaeodactylum tricornutum with different supply of inorganic carbon. Journal of applied phycology, 26, 131-139, (2014).

Deleted: ¶

Deleted: Pineau, B., Girard-Bascou, J., Eberhard, S., Choquet, Y., Trémolières, A., Gérard-Hirne, C., Bennardo-Connan, A., Decottignies, P., Gillet, S. and Wollman, F. A.: A single mutation that causes phosphatidylglycerol deficiency impairs synthesis of photosystem II cores in Chlamydomonas reinhardtii, Eur. J. Biochem., 271(2), 329–338, doi:10.1046/j.1432-1033.2003.03931.x, 2004.

Deleted: ¶

W., Plas, A. K. v. d., Yasuhara, M., Zhang, J., and Zhu, Z. Y.: System controls of coastal and open ocean oxygen depletion, Prog. Oceanogr., 197, 102613, https://doi.org/10.1016/j.pocean.2021.102613, 2021.

Poerschmann, J., Spijkerman, E. and Langer, U.: Fatty acid patterns in Chlamydomonas sp. as a marker for nutritional regimes and temperature under extremely acidic conditions, Microb. Ecol., 48(1), 78–89, doi:10.1007/s00248-003-0144-6, 2004.

Popendorf, K.J., Lomas, M.W. and Van Mooy, B.A.: Microbial sources of intact polar diacylglycerolipids in the Western North Atlantic Ocean. Organic geochemistry, 42(7), pp.803-811, https://doi.org/10.1016/j.orggeochem.2011.05.003, 2011.

Popko, J., Herrfurth, C., Feussner, K., Ischebeck, T., Iven, T., Haslam, R., Hamilton, M., Sayanova, O., Napier, J., Khozin-Goldberg, I. and Feussner, I.: Metabolome analysis reveals betaine lipids as major source for triglyceride formation, and the accumulation of sedoheptulose during nitrogen-starvation of Phaeodactylum tricornutum, PLoS One, 11(10), 1–23, doi:10.1371/journal.pone.0164673, 2016.

Raven, J. A., and Beardall, J.: Carbohydrate metabolism and respiration in algae, In Larkum, A. W. D., Douglas, S. S., Raven, J. A. (Eds) Photosynthesis in algae, 14, pp. 205-224, Springer, Dordrecht, https://doi.org/10/1007/978-94-007-1038-2_10, 2003.

Riebesell, U., Czerny, J., Von Bröckel, K., Boxhammer, T., Büdenbender, J., Deckelnick, M., Fischer, M., Hoffmann, D., Krug, S. A., Lentz, U., Ludwig, A., Muche, R. and Schulz, K. G.: Technical Note: A mobile sea-going mesocosm system - New opportunities for ocean change research, Biogeosciences, 10(3), 1835–1847, doi:10.5194/bg-10-1835-2013, 2013.

Roessler, P. G. Environmental control of glycerolipid metabolism in microalgae: commercial implications and future research directions, Journal of Phycology, 26.3, 393-399, https://doi.org/10/1111/j.0022-3646.1990.00383.x, 1990.

Russell, N. J., and Nichols, D. S.: Polyunsaturated fatty acids in marine bacteria—a dogma rewritten, Microbiology, 145.4, 767-779, doi:10.1099/13500872-145-4-767, 1999.

Rütters, H., Sass, H., Cypionka, H., and Rullkötter, J.: Monoalkylether phospholipids in the sulfate-reducing bacteria Desulfosarcina variabilis and Desulforhabdus amnigenus, Arch. Microbiol., 176, 435–442, doi: 10.1007/s002030100343, 2001.

Sakamoto, T. and Murata, N.: Regulation of the desaturation of fatty acids and its role in tolerance to cold and salt stress, Curr. Opin. Microbiol., 5(2), 206–210, doi:10.1016/S1369-5274(02)00306-5, 2002.

Sakurai, I., Hagio, M., Gombos, Z., Tyystjärvi, T., Paakkarinen, V., Aro, E. M. and Wada, H.: Requirement of Phosphatidylglycerol for Maintenance of Photosynthetic Machinery, Plant Physiol., 133(3), 1376–1384, doi:10.1104/pp.103.026955, 2003.

Sato, N. and Murata, N.: Temperature shift-induced responses in lipids in the blue-green alga, Anabaena variabilis, Biochim. Biophys. Acta - Lipids Lipid Metab., 619(2), 353–366, doi:10.1016/0005-2760(80)90083-1, 1980.

Sato, N., Aoki, M., Maru, Y., Sonoike, K., Minoda, A. and Tsuzuki, M.: Involvement of sulfoquinovosyl diacylglycerol in the structural integrity and heat-tolerance of photosystem II, Planta, 217(2), 245–251, doi:10.1007/s00425-003-0992-9, 2003.

Sayanova, O., Mimouni, V., Ulmann, L., Morant-Manceau, A., Pasquet, V., Schoefs, B. and Napier, J. A.: Modulation of lipid biosynthesis by stress in diatoms, Philos. Trans. R. Soc. B Biol. Sci., 372(1728), doi:10.1098/rstb.2016.0407, 2017.

Schubotz, F., Wakeham, S. G., Lipp, J. S., Fredricks, H. F. and Hinrichs, K. U.: Detection of microbial biomass by intact polar membrane lipid analysis in the water column and surface sediments of the Black Sea, Environ. Microbiol., 11(10), 2720–2734, doi:10.1111/j.1462-2920.2009.01999.x, 2009.

Schubotz, F., Xie, S., Lipp, J. S., Hinrichs, K. and Wakeham, S. G.: Intact polar lipids in the water column of the eastern tropical North Pacific: abundace and structural variety of non-phosphorus lipids, Biogeosciences, 15, 6481-6501, https://doi.org/10.5194/bg-15-6481-2018, 2018.

Sinensky, M.: Homeoviscous adaptation: a homeostatic process that regulates the viscosity of membrane lipids in Escherichia coli, Proc. Natl. Acad. Sci. U. S. A., 71(2), 522–525, doi:10.1073/pnas.71.2.522, 1974.

Singh, Y. and Kumar, H. D.: Lipid and hydrocarbon production by Botryococcus spp. under nitrogen limitation and anaerobiosis, World J. Microbiol. Biotechnol., 8(2), 121–124, doi:10.1007/BF01195829, 1992.

Smalley, G. W., Coats, D. W., and Stoecker, D. K.: Feeding in the mixotrophic dinoflagellate *Ceratium furca* is influenced by intracellular nutrient concentrations, Mar. Ecol. Prog. Ser., 262, 137-151, doi:10.3354/meps262137, 2003.

Speciale, G., Jin, Y., Davies, G. J., Williams, S. J. and Goddard-Borger, E. D.: YihQ is a sulfoquinovosidase that cleaves sulfoquinovosyl diacylglyceride sulfolipids, Nat. Chem. Biol., 12(4), 215–217, doi:10.1038/nchembio.2023, 2016.

Stramma, L., Johnson, G. C., Sprintall, J. and Mohrholz, V.: Expanding oxygen-minimum zones in the tropical oceans, Science , 320, 655–658, doi:10.1126/science.1153847, 2008.

Stramma, L., Schmidtko, S., Levin, L. A. and Johnson, G. C.: Ocean oxygen minima expansions and their biological impacts, Deep. Res. Part I Oceanogr. Res. Pap., 57(4), 587–595, doi:10.1016/j.dsr.2010.01.005, 2010.

Sturt, H. F., Summons, R. E., Smith, K., Elvert, M. and Hinrichs, K. U.: Intact polar membrane lipids in prokaryotes and sediments deciphered by high-performance liquid chromatography/electrospray ionization multistage mass spectrometry - New biomarkers for biogeochemistry and microbial ecology, Rapid Commun. Mass Spectrom., 18(6), 617–628, doi:10.1002/rcm.1378, 2004.

Sukenik, A., Zmora, O. and Carmeli, Y.: Biochemical quality of marine unicellular algae with special emphasis on lipid composition. II. Nannochloropsis sp., Aquaculture, 117(3–4), 313–326, doi:10.1016/0044-8486(93)90328-V, 1993.

Suzumura, M.: Phospholipids in marine environments: a review, Talanta, 66, 422–434, doi: 10.1016/j.talanta.2004.12.008, 2005.

Tatsuzawa, H. and Takizawa, E.: Fatty Acid and Lipid Composition of the Acidophilic green alga Chlamydomonas Sp., Journal of Phycology, 32(4), 598–601, https://doi.org/10.1111/j.0022-3646.1996.00598.x, 1996.

Taucher, J., Bach, L. T., Boxhammer, T., Nauendorf, A., Achterberg, E. P., Algueró-Muñiz, M., Arístegui, J., Czerny, J., Esposito, M., Guan, W., Haunost, M., Horn, H. G., Ludwig, A., Meyer, J., Spisla, C., Sswat, M., Stange, P., Riebesell, U., Aberle-Malzahn, N., Archer, S., Boersma, M., Broda, N., Büdenbender, J., Clemmesen, C., Deckelnick, M., Dittmar, T., Dolores-Gelado, M., Dörner, I., Fernández-Urruzola, I., Fiedler, M., Fischer, M., Fritsche, P., Gomez, M., Grossart,

Deleted: Schubotz, F.: Membrane Homeostasis upon Nutrient (C, N, P) Limitation, Biog. Fat. Acids, Lipids Membr., 823–847, doi:10.1007/978-3-319-50430-8_59, 2019.

Deleted: ¶

Deleted: Schulz, K. G. and Riebesell, U.: Diurnal changes in seawater carbonate chemistry speciation at increasing atmospheric carbon dioxide, Mar. Biol., 160(8), 1889–1899, doi:10.1007/s00227-012-1965-y, 2013.

Deleted: ¶

Deleted: Sharp, J. H.: Improved analysis for "particulate" organic carbon and nitrogen from seawater, Limnol. Oceanogr., 19(6), 984–989, doi:10.4319/lo.1974.19.6.0984, 1974.

Deleted: ¶

Deleted: Simionato, D., Block, M. A., La Rocca, N., Jouhet, J., Maréchal, E., Finazzi, G. and Morosinotto, T.: The response of Nannochloropsis gaditana to nitrogen starvation includes de novo biosynthesis of triacylglycerols, a decrease of chloroplast galactolipids, and reorganization of the photosynthetic apparatus, Eukaryot. Cell, 12(5), 665–676, doi:10.1128/EC.00363-12, 2013.…

Deleted: ¶

Formatted: Font: (Default) Times New Roman, 10 pt

Formatted: Font: (Default) Times New Roman, 10 pt, Italic

Formatted: Font: (Default) Times New Roman, 10 pt

H. P., Hattich, G., Hernández-Brito, J., Hernández-Hernández, N., Hernández-León, S., Hornick, T., Kolzenburg, R., Krebs, L., Kreuzburg, M., Lange, J. A. F., Lischka, S., Linsenbarth, S., Löscher, C., Martínez, I., Montoto, T., Nachtigall, K., Osma-Prado, N., Packard, T., Pansch, C., Posman, K., Ramírez-Bordón, B., Romero-Kutzner, V., Rummel, C., Salta, M., Martínez-Sánchez, I., Schröder, H., Sett, S., Singh, A., Suffrian, K., Tames-Espinosa, M., Voss, M., Walter, E., Wannicke, N., Xu, J. and Zark, M.: Influence of ocean acidification and deep water upwelling on oligotrophic plankton communities in the subtropical North Atlantic: Insights from an in situ mesocosm study, Front. Mar. Sci., 4(APR), doi:10.3389/fmars.2017.00085, 2017.

Thamdrup, B., Dalsgaard, T. and Revsbech, N. P.: Widespread functional anoxia in the oxygen minimum zone of the Eastern South Pacific, Deep. Res. Part I Oceanogr. Res. Pap., 65, 36–45, doi:10.1016/j.dsr.2012.03.001, 2012.

Tréguer, P., Bowler, C., Moriceau, B., Dutkiewicz, S., Gehlen, M., Aumont, O., Bittner, L., Dugdale, R., Finkel, Z., Iudicone, D., Jahn, O., Guidi, L., Lasbleiz, M., Leblanc, K., Levy, M., and Pondaven, P.: Influence of diatom diversity on the ocean biological carbon pump. Nature Geosci, 11, 27–37, doi: https://doi.org/10.1038/s41561-017-0028-x, 2018.

Tretkoff, E. Research Spotlight: Coastal cooling and marine productivity increasing off Peru. Eos Transact. Am. Geophys. Union 92, 184–184. doi: 10.1029/2011eo210009, 2011

Twining, C. W., Taipale, S. J., Ruess, L., Bec, A., Martin-Creuzburg, D. and Kainz, M. J.: Stable isotopes of fatty acids: Current and future perspectives for advancing trophic ecology, Philos. Trans. R. Soc. B Biol. Sci., 375(1804), doi:10.1098/rstb.2019.0641, 2020.

Tyralis, H., Papacharalampous, G., & Langousis, A. A brief review of random forests for water scientists and practitioners and their recent history in water resources. Water, 11(5), 910, https://doi.org/10.3390/w11050910, 2019.

Ulloa, O. and Pantoja, S.: The oxygen minimum zone of the eastern South Pacific, Deep. Res. Part II Top. Stud. Oceanogr., 56(16), 987–991, doi:10.1016/j.dsr2.2008.12.004, 2009.

Van Mooy, B. A. S. and Fredricks, H. F.: Bacterial and eukaryotic intact polar lipids in the eastern subtropical South Pacific: Water-column distribution, planktonic sources, and fatty acid composition, Geochim. Cosmochim. Acta, 74(22), 6499–6516, doi:10.1016/j.gca.2010.08.026, 2010.

Van Mooy, B. A. S., Fredricks, H. F., Pedler, B. E., Dyhrman, S. T., Karl, D. M., Koblížek, M., Lomas, M. W., Mincer, T. J., Moore, L. R., Moutin, T., Rappé, M. S. and Webb, E. A.: Phytoplankton in the ocean use non-phosphorus lipids in response to phosphorus scarcity, Nature, 458(7234), 69–72, doi:10.1038/nature07659, 2009.

Van Mooy, B. A., Rocap, G., Fredricks, H. F., Evans, C. T., and Devol, A. H.: Sulfolipids dramatically decrease phosphorus demand by picocyanobacteria in oligotrophic marine environments, P. Natl. Acad. Sci. USA, 103(23), 8607–8612, https://doi.org/10.1073/pnas.0600540103, 2006.

Vargas, C. A., Cantarero, S. I., Sepúlveda, J. A., Galán, A., De Pol Holz, R., Walker, B., Schneider, W., Farías, L., Cornejo D'Ottone, M., Walker, J., Xu, X., and Salisbury, J.: A source of isotopically light organic carbon in a low-pH anoxic marine zone. Nature Communications, 12, 1604. https://doi.org/10.1038/s41467-021-21871-4, 2021.

Volkman, J. K.,

Deleted: Tyralis, H. and Papacharalampous, G.: Scientists and Practitioners and Their Recent History, Water, 2019.

Deleted: Missing: Vargas et al 2021, from section 4.2.2. pHT and Inorganic C availabilty

Deleted: ¶

Jeffrey, S. W., Nichols, P. D., Rogers, G. I. and Garland, C. D.: Fatty acid and lipid composition of 10 species of microalgae used in mariculture, J. Exp. Mar. Bio. Ecol., 128(3), 219–240, doi:10.1016/0022-0981(89)90029-4, 1989.

Volkman, J. K., Barrett, S. M., Blackburn, S. I., Mansour, M. P., Sikes, E. L. and Gelin, F.: Microalgal biomarkers: A review of recent research developments, Org. Geochem., 29(5-7–7 pt 2), 1163–1179, doi:10.1016/S0146-6380(98)00062-X, 1998.

Wada, H., and Murata, N.: Lipids in thylakoid membranes and photosynthetic cells, In: Lipids in Photosynthesis, Springer, Dordrecht, 1-9, https;//doi.org/10.1007/978-90-481-2862-1_1, 2009.

Wagner, S., Schubotz, F., Kaiser, K., Hallmann, C., Waska, H., Rossel, P. E., Hansman, R., Elvert, M., Middelburg, J. J., Engel, A., Blattmann, T. M., Catalá, T. S., Lennartz, S. T., Gomez-Saez, G. V., Pantoja-Gutiérrez, S., Bao, R. and Galy, V.: Soothsaying DOM: A Current Perspective on the Future of Oceanic Dissolved Organic Carbon, Front. Mar. Sci., 7(May), 1–17, doi:10.3389/fmars.2020.00341, 2020.

Wakeham, S. G., Turich, C., Schubotz, F., Podlaska, A., Li, X. N., Varela, R., Astor, Y., Sáenz, J. P., Rush, D., Sinninghe Damsté, J. S., Summons, R. E., Scranton, M. I., Taylor, G. T. and Hinrichs, K. U.: Biomarkers, chemistry and microbiology show chemoautotrophy in a multilayer chemocline in the Cariaco Basin, Deep. Res. Part I Oceanogr. Res. Pap., 63, 133–156, doi:10.1016/j.dsr.2012.01.005, 2012.

Wang, X., Shen, Z. and Miao, X.: Nitrogen and hydrophosphate affects glycolipids composition in microalgae, Sci. Rep., 6(July), 1–9, doi:10.1038/srep30145, 2016.

Wilhelm, C., Jungandreas, A., Jakob, T. and Goss, R.: Light acclimation in diatoms: From phenomenology to mechanisms, Mar. Genomics, 16(1), 5–15, doi:10.1016/j.margen.2013.12.003, 2014.

Wörmer, L., Lipp, J. S., Schröder, J. M., Hinrichs, K. U.:Application of two new LC–ESI–MS methods for improved detection of intact polar lipids (IPLs) in environmental samples, Org. Geochem., 59, 10-21, https://doi.org/10.1016/j.orggeochem.2013.03.004, 2013.

Wörmer, L., Lipp, J. S., and Hinrichs, K. U.: Comprehensive analysis of microbial lipids in environmental samples through HPLC-MS protocols, in: Hydrocarbon and lipid microbiology protocols, Springer, Berlin, Heidelber, 289-317, https://doi.org/10.1007/8623_2015_183, 2015.

Wright, J. J., Konwar, K. M. and Hallam, S. J.: Microbial ecology of expanding oxygen minimum zones, Nat. Rev. Microbiol., 10(6), 381–394, doi:10.1038/nrmicro2778, 2012.

Wu, R. S. S., Wo, K. T. and Chiu, J. M. Y.: Effects of hypoxia on growth of the diatom Skeletonema costatum, J. Exp. Mar. Bio. Ecol., 420–421, 65–68, doi:10.1016/j.jembe.2012.04.003, 2012.

Wyrtki, K.: The oxygen minima in relation to ocean circulation, Deep. Res. Oceanogr. Abstr., 9(1–2), 11–23, doi:10.1016/0011-7471(62)90243-7, 1962.

Yang, C., Boggasch, S., Haase, W. and Paulsen, H.: Thermal stability of trimeric light-harvesting chlorophyll a/b complex (LHCIIb) in liposomes of thylakoid lipids, Biochim. Biophys. Acta - Bioenerg., 1757(12), 1642–1648, doi:10.1016/j.bbabio.2006.08.010, 2006.

Deleted: Wada, H., Combos, Z. and Murata, N.: Enhancement of chilling tolerance of a cyanobacterium by genetic manipulation of fatty acid desaturation, Nature, 347(6289), 200–203, doi:10.1038/347200a0, 1990.

Deleted: ¶

Yang, K. and Han, X.: Accurate quantification of lipid species by electrospray ionization mass spectrometry - Meets a key challenge in lipidomics, Metabolites, 1(1), 21–40, doi:10.3390/metabo1010021, 2011.

Yang, W., Catalanotti, C., Wittkopp, T. M., Posewitz, M. C. and Grossman, A. R.: Algae after dark: Mechanisms to cope with anoxic/hypoxic conditions, Plant J., 82(3), 481–503, doi:10.1111/tpj.12823, 2015.

Yeesang, C. and Cheirsilp, B.: Effect of nitrogen, salt, and iron content in the growth medium and light intensity on lipid production by microalgae isolated from freshwater sources in Thailand, Bioresour. Technol., 102(3), 3034–3040, doi:10.1016/j.biortech.2010.10.013, 2011.

Yoon, K., Han, D., Li, Y., Sommerfeld, M. and Hu, Q.: Phospholipid:Diacylglycerol acyltransferase is a multifunctional enzyme involved in membrane lipid turnover and degradation while synthesizing triacylglycerol in the unicellular green microalga chlamydomonas reinhardtii, Plant Cell, 24(9), 3708–3724, doi:10.1105/tpc.112.100701, 2012.

Yvon-Durocher, G., Allen, A. P., Cellamare, M., Dossena, M., Gaston, K. J., Leitao, M., Montoya, J. M., Reuman, D. C., Woodward, G. and Trimmer, M.: Five Years of Experimental Warming Increases the Biodiversity and Productivity of Phytoplankton, PLoS Biol., 13(12), 1–22, doi:10.1371/journal.pbio.1002324, 2015.

Zienkiewicz, K., Du, Z. Y., Ma, W., Vollheyde, K. and Benning, C.: Stress-induced neutral lipid biosynthesis in microalgae — Molecular, cellular and physiological insights, Biochim. Biophys. Acta - Mol. Cell Biol. Lipids, 1861(9), 1269–1281, doi:10.1016/j.bbalip.2016.02.008, 2016.

Zink K-G, Wilkes H, Disko U, Elvert M, Horsfield B. Intact phospholipids—microbial "life markers" in marine deep subsurface sediments. Org. Geochem; 34: 755-769, https://doi.org/10.1016/S0146-6380(03)00041-X, 2003.

Tables

Table 1: Concentration of inorganic nutrients (µmol/L), nutrient stoichiometry, and pH$_T$ of the two batches of ODZ water collected and added to the mesocosm experiment.

Deleted: s

Formatted: Subscript

Deleted: . Values

Deleted: includ

Deleted: e

Deleted: ing dissolved silicate, phosphate, nitrite, ammonium, nitrate, and the associated N:P:Si and pH

Deleted: T

Deleted: in the two deep water batches

Deleted: used

Deleted: before the addition of ODZ water

Deleted: in this

	$Si(OH)_4$	PO_4^{3-}	NO_2^-	NH_4^+	NO_3^-	N:P:Si	pHT	Depth (m)
Station 1	17.4	2.6	0	0.3	0	0.1:1.0:6.7	7.47	30
Station 3	19.6	2.5	2.9	0.3	1.1	1.7:1.0:7.8	7.49	70

Stations	$Si(OH)_4$	PO_4^{3-}	NO_2^-	NH_4^+	NO_3^-	N:P:Si	pH	Depth (m)
Station 1	17.4	2.6	0	0.3	0	0.1:1.0:6.7	7.47	30
Station 3	19.6	2.5	2.9	0.3	1.1	1.7:1.0:7.8	7.49	70

Table 2: IPL classes included in this study and their respective acronyms.

Deleted: ese analyses

IPL Headgroups	Acronym	IPL Category
Digalactosyldiacylglycerol	DG	Glycolipid
Monogalactosyldiacylglycerol	MG	Glycolipid
Sulfoquinovosyl	SQ	Glycolipid
Phosphatidylglycerol	PG	Phospholipid
Phosphatidylcholine	PC	Phospholipid
Phosphatidylethanolamine	PE	Phospholipid
Diacylglyceryl trimethylhomoserine	DGTS	Betaine Lipid
Diacylglyceryl hydroxymethyl-trimethyl-beta-alanine	DGTA	Betaine Lipid
Diacylglyceryl carboxyhydroxymethylcholine	DGCC	Betaine Lipid

IPL Headgroups	Acronym	IPL Classes
Sulfoquinovosyl	SQ	Glycolipid
Monogalactosyldiacylglycerol	MG	Glycolipid
Digalactosyldiacylglycerol	DG	Glycolipid
Phosphatidylglycerol	PG	Phospholipid
Phosphatidylethanolamine	PE	Phospholipid
Phosphatidylcholine	PC	Phospholipid
Diacylglyceryl trimethylhomoserine	DGTS	Betaine Lipid
Diacylglyceryl hydroxymethyl-trimethyl-beta-alanine	DGTA	Betaine Lipid
Diacylglyceryl carboxyhydroxymethylcholine	DGCC	Betaine Lipid

2490 **Figures**

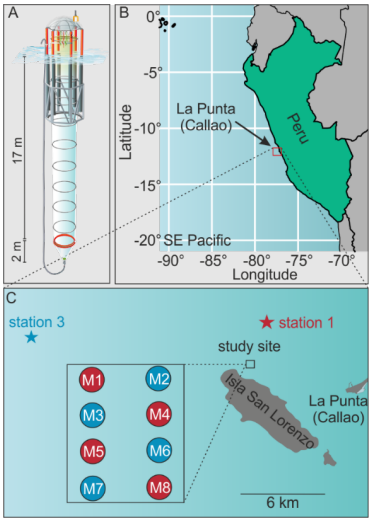

2491

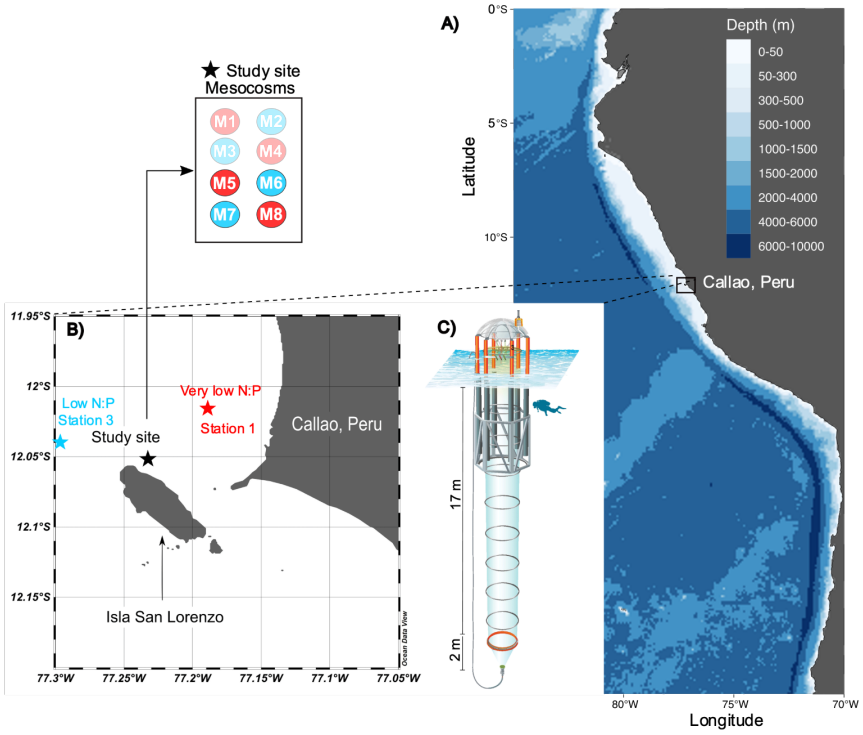

Figure 1: The KOSMOS study site. (A) Overview map indicating the location of the study region in La Punta, Callao, Perú. (B) Detailed map of the study site with the mesocosm arrangement (M1-8). Red (very low N:P) and blue (low N:P) colors indicate the different stations for ODZ water collection (1 and 3; star symbols) and replicates of the two different water treatments (numbers in circles in insert). (C) Diagram of a mesocosm unit with underwater bag dimensions. Modified figure from Chen et al. (2022).

Deleted: Diagram of a mesocosm unit with underwater bag dimensions.…

Deleted: The stars mark the locations of stations 1 and 3, where the two different ODZ water masses were collected.…

Deleted: (B) Overview map indicating the location of the study region in La Punta, Callao, Perú.

Deleted: Detailed map of the study site with the mesocosm arrangement (M1-8). Red and blue colors indicate the replicates of the two different water treatments. The stars mark the locations of stations 1 and 3, where the two different OMZ water masses were collected.…

Deleted: F

Deleted: Bach

Deleted: 0

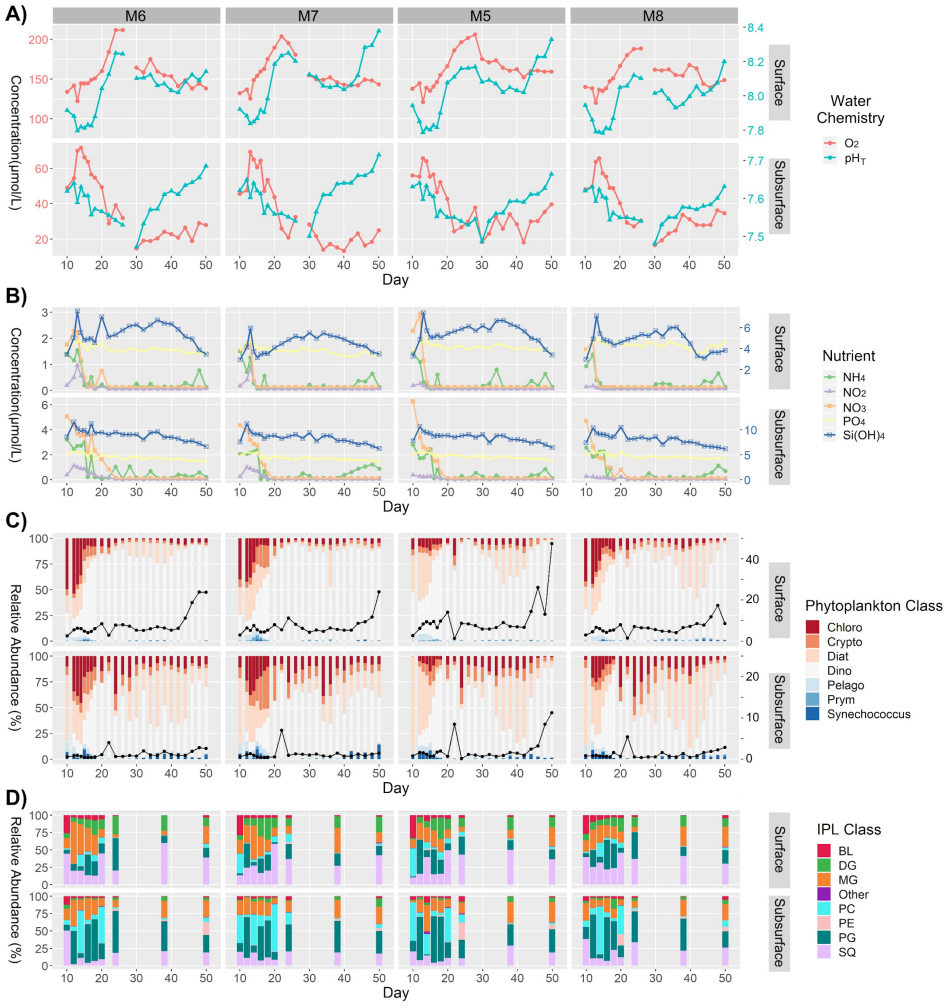
A)
M6
M7
M5
M8
Surface
Subsurface
Concentration(µmol/L)
Day
Water Chemistry
O2
pHT
B)
Nutrient
NH4
NO2
NO3
PO4
Si(OH)4
C)
Relative Abundance (%)
Phytoplankton Class
Chloro
Crypto
Diat
Dino
Pelago
Prym
Synechococcus
D)
IPL Class
BL
DG
MG
Other
PC
PE
PG
SQ

2516

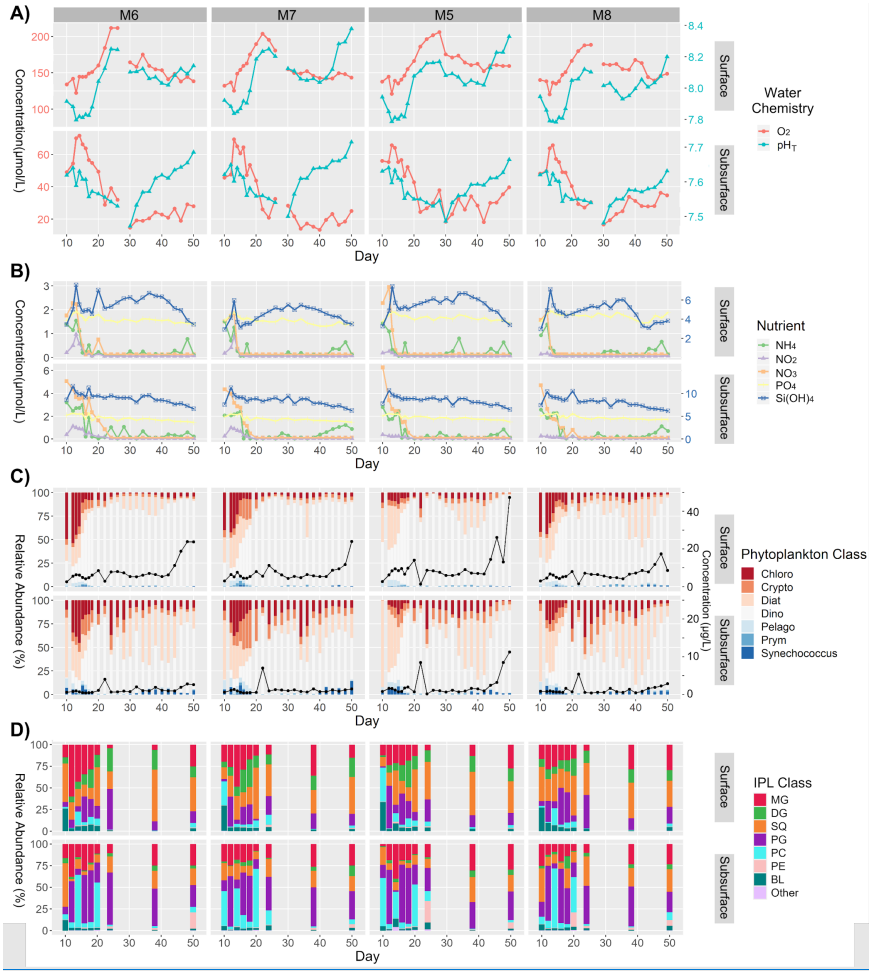

Figure 2: Summary of major physicochemical, biological, and lipidomic measurements in surface and subsurface waters of mesocosms analyzed in this study from the time of deep-water injection to the end of the experiment. A) Concentration of O_2 (µmol/L; left Y axis), and pH_T (total scale; right Y axis). B) Concentration of inorganic N (left Y axis), P (left Y axis), and $Si(OH)_4$ (right Y axis) expressed in µmol/L. C) Relative abundance (%) of phytoplankton classes (left Y axis) as well as total chl-a concentrations expressed in µg/L (black line; right Y axis). D) Relative abundance (%) of major IPL classes based on headgroup contributions to the total IPL pool.

Commented [6]: Requires C) right y-axis label for chl-a ug/L (black line)

Deleted:

Deleted: over the course of

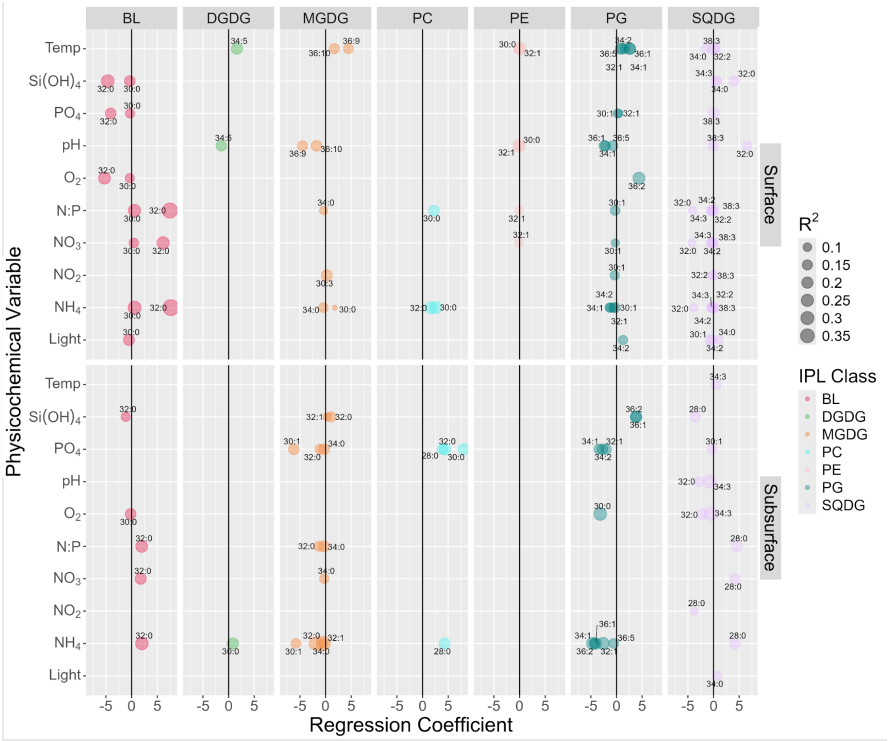

Figure 3: Summary of multiple linear regression analysis between the abundances of major IPL molecules (> 2.5% of total IPL pool) and physicochemical parameters showing only statistically significant ($p < 0.05$) linear responses after controlling for false discovery rate using a 0.1 alpha cutoff on adjusted p-values. The size of circles indicates the magnitude of the linear regression adjusted R^2. The upper and lower panels represent surface and subsurface waters, respectively. Numbers next to circles indicate the total number of carbon atoms and double bonds in core fatty acids chains.

Deleted: and

Deleted: by applying

Deleted: S

Deleted: U

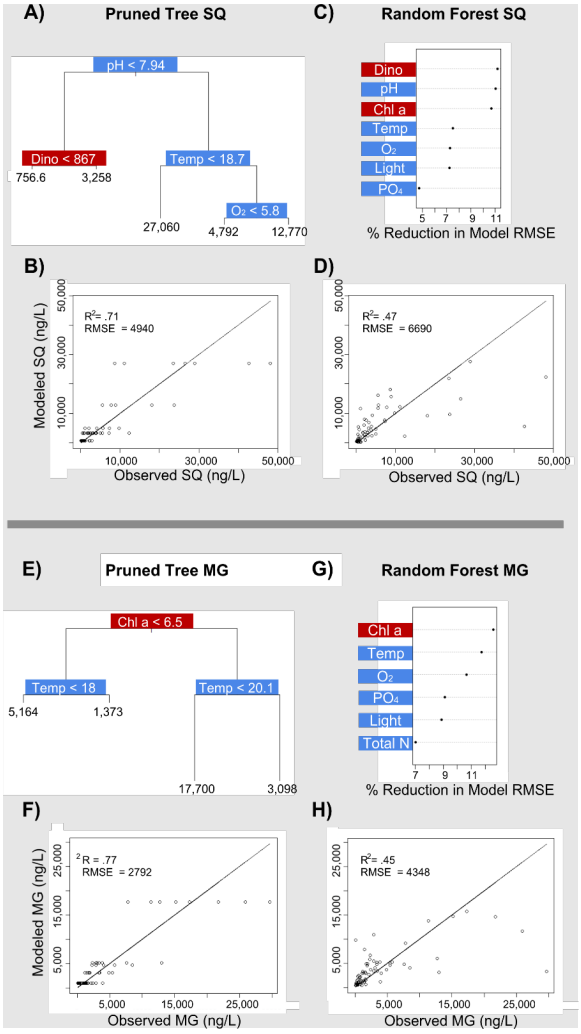

Figure 4: Classification and Regression Tree (CART) and Random Forest analyses of selected IPL classes (Top: SQ; Bottom: MG). A and E indicate a summary of primary predictors in the best fit CART (i.e. Pruned Tree), whereas B and F show model performance via adjusted R^2 and RMSE. C and G display Random Forest variable importance in the prediction of IPL classes as

defined by % reduction in RMSE, whereas D and H show model performance via adjusted R^2 and RMSE. Environmental variables are depicted in blue, whereas biological variables are shown in red for both analyses.

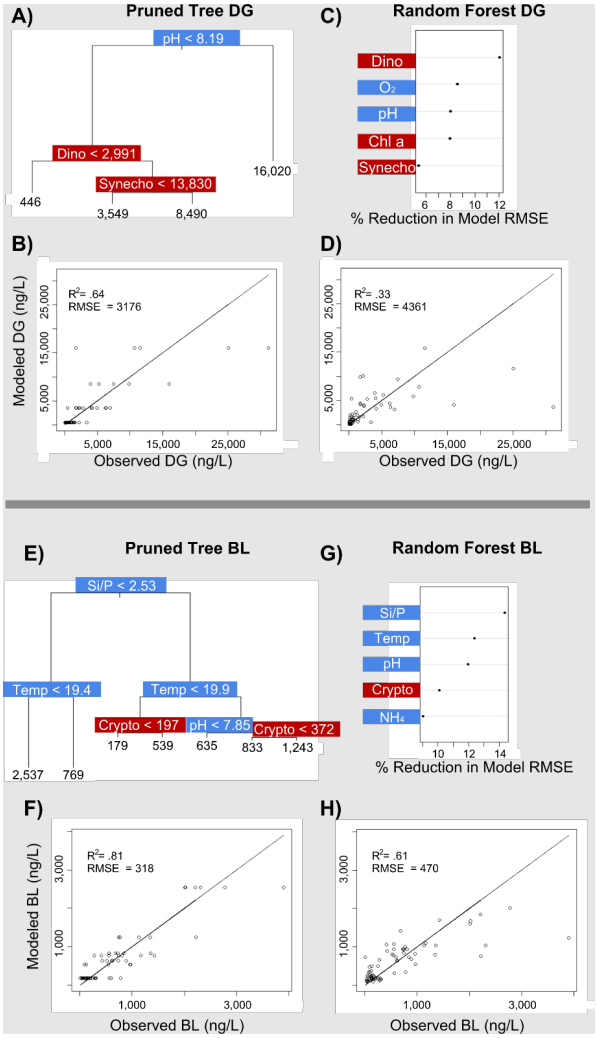

Figure 5: Classification and Regression Tree (CART) and Random Forest analyses of selected IPL classes (Top: DG; Bottom: BL). A and E indicate a summary of primary predictors in the best fit CART (i.e. Pruned Tree), whereas B and F show model performance via adjusted R^2 and RMSE. C and G display Random Forest variable importance in the prediction of IPL classes as defined by % reduction in RMSE, whereas D and H show model performance via adjusted R^2 and RMSE. Environmental variables are depicted in blue, whereas biological variables are shown in red for both analyses.

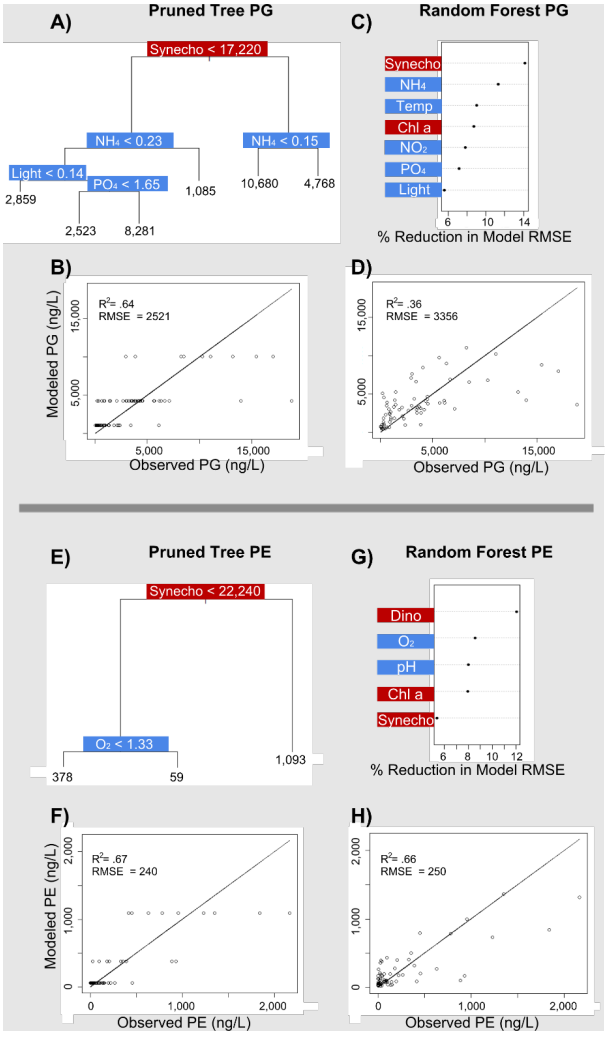

Figure 6: Classification and Regression Tree (CART) and Random Forest analyses of selected IPL classes (Top: PG; Bottom: PE). A and E indicate a summary of primary predictors in the best fit CART (i.e. Pruned Tree), whereas B and F show model performance via adjusted R^2 and RMSE. C and G display Random Forest variable importance in the prediction of IPL classes as

defined by % reduction in RMSE, whereas D and H show model performance via adjusted R^2 and RMSE. Environmental variables are depicted in blue, whereas biological variables are shown in red for both analyses.

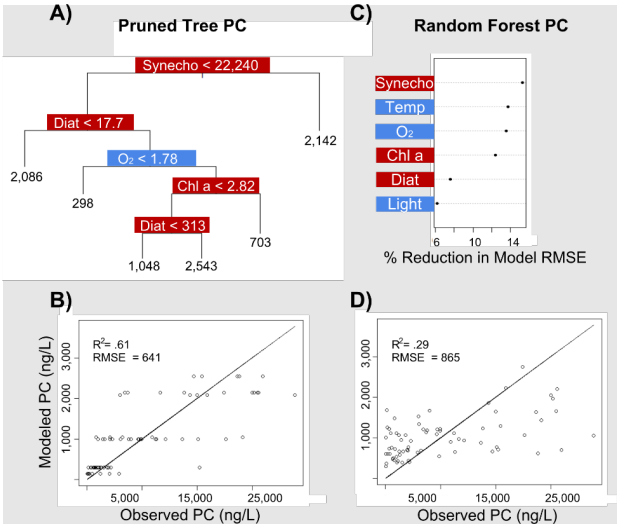

Figure 7: Classification and Regression Tree (CART) and Random Forest analyses of selected IPL classes (PC). A indicate a summary of primary predictors in the best fit CART (i.e. Pruned Tree), whereas B shows model performance via adjusted R^2 and RMSE. C and G display Random Forest variable importance in the prediction of IPL classes as defined by % reduction in RMSE, whereas D show model performance via adjusted R^2 and RMSE. Environmental variables are depicted in blue, whereas biological variables are shown in red for both analyses.

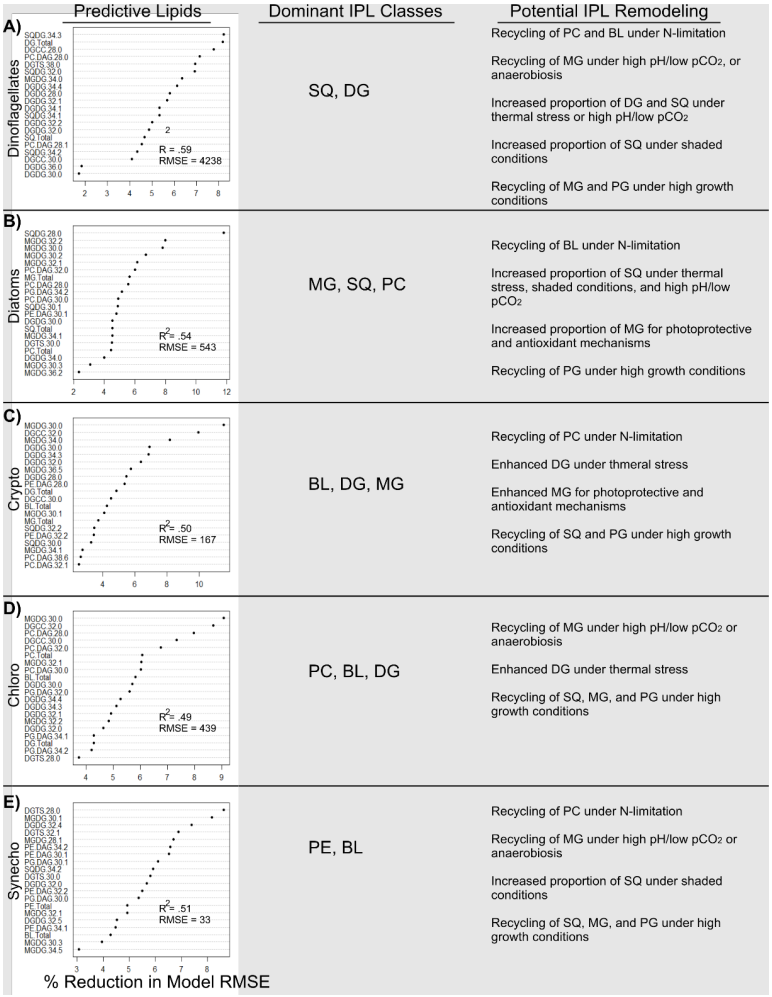
Predictive Lipids
Dominant IPL Classes
Potential IPL Remodeling
A)
Dinoflagellates
SQDG.34.3
DG Total
DGCC.28.0
PC.DAG.28.0
DGTS.38.0
SQDG.32.0
MGDG.34.0
DGDG.34.4
DGDG.28.0
DGDG.32.1
DGDG.34.1
SQDG.34.1
DGDG.32.2
DGDG.32.0
SQ Total
PC.DAG.28.1
SQDG.34.2
DGCC.30.0
DGDG.36.0
DGDG.30.0
R = .59
RMSE = 4238
2 3 4 5 6 7 8
SQ, DG
Recycling of PC and BL under N-limitation
Recycling of MG under high pH/low pCO2, or anaerobiosis
Increased proportion of DG and SQ under thermal stress or high pH/low pCO2
Increased proportion of SQ under shaded conditions
Recycling of MG and PG under high growth conditions
B)
Diatoms
SQDG.28.0
MGDG.32.2
MGDG.30.0
MGDG.30.2
MGDG.32.1
PC.DAG.32.0
MG Total
PC.DAG.28.0
PG.DAG.34.2
PC.DAG.30.0
SQDG.30.1
PE.DAG.30.1
DGDG.30.0
SQ Total
MGDG.34.1
DGTS.30.0
PC Total
DGDG.34.0
MGDG.30.3
MGDG.36.2
R2 = .54
RMSE = 543
2 4 6 8 10 12
MG, SQ, PC
Recycling of BL under N-limitation
Increased proportion of SQ under thermal stress, shaded conditions, and high pH/low pCO2
Increased proportion of MG for photoprotective and antioxidant mechanisms
Recycling of PG under high growth conditions
C)
Crypto
MGDG.30.0
DGCC.32.0
MGDG.34.0
DGDG.30.0
DGDG.34.3
DGDG.32.0
MGDG.36.5
DGDG.28.0
PE.DAG.28.0
DG Total
DGCC.30.0
BL Total
MGDG.30.1
MG Total
SQDG.32.2
PE.DAG.32.2
SQDG.30.0
MGDG.34.1
PC.DAG.38.6
PC.DAG.32.1
R2 = .50
RMSE = 167
4 6 8 10
BL, DG, MG
Recycling of PC under N-limitation
Enhanced DG under thmeral stress
Enhanced MG for photoprotective and antioxidant mechanisms
Recycling of SQ and PG under high growth conditions
D)
Chloro
MGDG.30.0
DGCC.32.0
PC.DAG.28.0
DGCC.30.0
PC.DAG.32.0
PC Total
MGDG.32.1
PC.DAG.30.0
BL Total
DGDG.30.0
PG.DAG.32.0
DGDG.34.4
DGDG.34.3
DGDG.32.1
MGDG.32.2
DGDG.32.0
PG.DAG.34.1
DG Total
PG.DAG.34.2
DGTS.28.0
R2 = .49
RMSE = 439
4 5 6 7 8 9
PC, BL, DG
Recycling of MG under high pH/low pCO2 or anaerobiosis
Enhanced DG under thermal stress
Recycling of SQ, MG, and PG under high growth conditions
E)
Synecho
DGTS.28.0
MGDG.30.1
DGDG.32.4
DGTS.32.1
MGDG.28.1
PE.DAG.34.2
PE.DAG.30.1
PG.DAG.30.1
SQDG.34.2
DGTS.30.0
DGDG.32.0
PE.DAG.32.2
PG.DAG.30.0
PE Total
MGDG.32.1
DGDG.32.2
PE.DAG.34.1
BL Total
MGDG.30.3
MGDG.34.5
R2 = .51
RMSE = 33
3 4 5 6 7 8
PE, BL
Recycling of PC under N-limitation
Recycling of MG under high pH/low pCO2 or anaerobiosis
Increased proportion of SQ under shaded conditions
Recycling of SQ, MG, and PG under high growth conditions
% Reduction in Model RMSE

2562

	Predictive Lipids	Dominant IPL Classes	Potential IPL Remodeling
A) Dinoflagellates	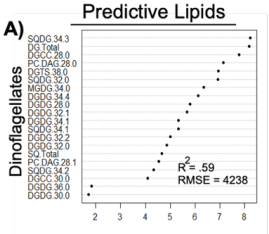	SQ, DG	Recycling of PC and BL under N-limitation Recycling of MG under high pH/low pCO_2, or anaerobiosis Increased proportion of DG and SQ under thermal stress or high pH/low pCO_2 Increased proportion of SQ under shaded conditions Recycling of MG and PG under high growth conditions
B) Diatoms	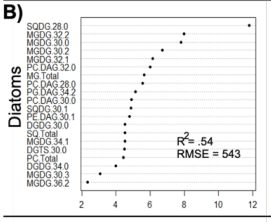	MG, SQ, PC	Recycling of BL under N-limitation Increased proportion of SQ under thermal stress, shaded conditions, and high pH/low pCO_2 Increased proportion of MG for photoprotective and antioxidant mechanisms Recycling of PG under high growth conditions
C) Crypto	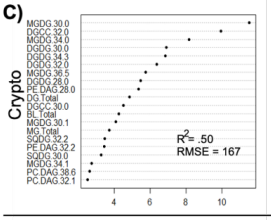	BL, DG, MG	Recycling of PC under N-limitation Enhanced DG under thmeral stress Enhanced MG for photoprotective and antioxidant mechanisms Recycling of SQ and PG under high growth conditions
D) Chloro	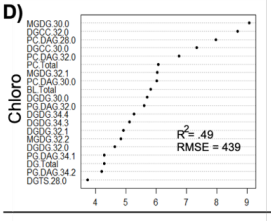	PC, BL, DG	Recycling of MG under high pH/low pCO_2 or anaerobiosis Enhanced DG under thermal stress Recycling of SQ, MG, and PG under high growth conditions
E) Synecho	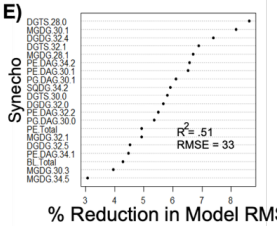	PE, BL	Recycling of PC under N-limitation Recycling of MG under high pH/low pCO_2 or anaerobiosis Increased proportion of SQ under shaded conditions Recycling of SQ, MG, and PG under high growth conditions

% Reduction in Model RMSE

2563

Figure 8: Random Forest-based identification of the 15 most important individual IPLs in the prediction of phytoplankton groups. Dominant IPL classes and the potential remodeling advantages for each group are summarized. The nomenclature of IPL molecules follows that of the main text, starting with the type of headgroup, followed by the number of carbon atoms in fatty acid chains, and the total number of double bonds in the fatty acid chains. The root mean square error (RMSE) of random forest models is defined as ng/L of chl-a, and coefficient of determination (R^2) provided for each model fit.

Deleted:

Deleted: molecules or classes

Deleted: classes

Deleted: are denoted by

Deleted: ir

Deleted: abbreviation

Deleted: final number refers to the

Deleted: unsaturations

Deleted: R

Page 19: [1] Deleted **Sebastian Ignacio Cantarero** **5/4/24 8:30:00 PM**

Page 19: [1] Deleted **Sebastian Ignacio Cantarero** **5/4/24 8:30:00 PM**

Page 19: [2] Deleted **Sebastian Ignacio Cantarero** **5/4/24 8:30:00 PM**

Page 19: [2] Deleted **Sebastian Ignacio Cantarero** **5/4/24 8:30:00 PM**

Page 19: [3] Formatted **Sebastian Ignacio Cantarero** **5/4/24 8:39:00 PM**

Subscript

Page 19: [4] Deleted **Sebastian Ignacio Cantarero** **5/4/24 8:59:00 PM**

Page 19: [5] Deleted **Sebastian Ignacio Cantarero** **5/4/24 8:38:00 PM**

Page 19: [6] Deleted **Sebastian Ignacio Cantarero** **6/8/24 3:54:00 PM**

Page 19: [7] Deleted **Sebastian Ignacio Cantarero** **6/8/24 4:01:00 PM**

Page 19: [8] Deleted **Sebastian Ignacio Cantarero** **5/4/24 9:13:00 PM**

Page 19: [9] Deleted **Sebastian Ignacio Cantarero** **5/4/24 9:12:00 PM**

Page 19: [10] Deleted **Sebastian Ignacio Cantarero** **5/4/24 9:19:00 PM**

Page 19: [11] Formatted **Sebastian Ignacio Cantarero** **5/5/24 7:33:00 PM**

Font: Italic

Page 19: [12] Formatted **Sebastian Ignacio Cantarero** **6/8/24 4:34:00 PM**

Subscript

Page 19: [13] Formatted **Sebastian Ignacio Cantarero** **6/8/24 4:35:00 PM**

Subscript

Page 19: [14] Deleted **Sebastian Ignacio Cantarero** **6/8/24 4:33:00 PM**

Page 19: [15] Deleted **Sebastian Ignacio Cantarero** **5/4/24 9:32:00 PM**

Page 19: [15] Deleted **Sebastian Ignacio Cantarero** **5/4/24 9:32:00 PM**

Page 20: [16] Deleted **Sebastian Ignacio Cantarero** **5/5/24 7:44:00 PM**

Page 20: [16] Deleted **Sebastian Ignacio Cantarero** **5/5/24 7:44:00 PM**

Page 20: [17] Deleted **Sebastian Ignacio Cantarero** **5/5/24 7:44:00 PM**

Page 20: [18] Deleted **Sebastian Ignacio Cantarero** **5/5/24 7:44:00 PM**

Page 20: [19] Commented [1] **Harry Allbrook** **5/6/24 9:12:00 AM**

RC2-26: L 608-609 – I suggest that the authors consider why dinoflagellates are more dominant in the surface layer. Dinoflagellates are possibly mixotrophic, some are also heterotrophic, while diatoms are probably limited by Si availability.

Response RC2-26: Whereas we briefly address this point in section 4.3.1, we plan to expand on it in this particular section of the manuscript as suggested. Namely, we will discuss that mixotrophic dinoflagellates scavenging N from the PON pool likely grants them a considerable advantage in N-depleted surface waters. Their presence in the KOSMOS 2017 experiment, particularly in the final phases, has been reported by Bach et al. (2020) and Min et al. (2023).

We will include the recent publication in our references:

Min, M.A., Needham, D.M., Sudek, S., Truelove, N.K., Pitz, K.J., Chavez, G.M., Poirier, C., Gardeler, B., von der Esch, E., Ludwig, A., Riebesell, U., Worden, A.Z., Chavez, F.P., 2023. Ecological divergence of a mesocosm in an eastern boundary upwelling system assessed with multi-marker environmental DNA metabarcoding. Biogeosciences 20, 1277–1298. https://doi.org/10.5194/bg-20-1277-2023

Page 20: [20] Deleted **Julio Sepúlveda** **6/10/24 6:28:00 PM**

Page 20: [20] Deleted **Julio Sepúlveda** **6/10/24 6:28:00 PM**

Page 20: [21] Deleted **Julio Sepúlveda** **6/10/24 6:28:00 PM**

Page 20: [22] Formatted **Sebastian Ignacio Cantarero** **5/5/24 7:39:00 PM**

Subscript

Page 20: [23] Commented [4] **Harry Allbrook** **5/5/24 9:35:00 PM**

I think wording in that this is the hypothesis from the dataset discussed could aid the TAG reviewer comments

Page 20: [24] Formatted **Sebastian Ignacio Cantarero** **5/5/24 7:53:00 PM**

Subscript

Page 20: [25] Deleted **Sebastian Ignacio Cantarero** **5/5/24 7:54:00 PM**

Page 20: [26] Formatted **Sebastian Ignacio Cantarero** **6/8/24 4:46:00 PM**

Subscript

Page 20: [27] Formatted **Sebastian Ignacio Cantarero** **6/8/24 4:46:00 PM**

Subscript

Page 20: [28] Deleted **Sebastian Ignacio Cantarero** **5/5/24 8:07:00 PM**

Page 20: [29] Deleted **Sebastian Ignacio Cantarero** **5/5/24 8:24:00 PM**

Page 24: [30] Deleted **Sebastian Ignacio Cantarero** **5/5/24 9:35:00 PM**

Page 24: [31] Deleted **Julio Sepúlveda** **6/10/24 6:54:00 PM**

Page 24: [32] Deleted **Sebastian Ignacio Cantarero** **5/5/24 9:35:00 PM**

Page 24: [33] Deleted **Sebastian Ignacio Cantarero** **5/5/24 9:25:00 PM**

Page 24: [34] Deleted **Sebastian Ignacio Cantarero** **5/5/24 9:25:00 PM**

Page 28: [35] Deleted **Julio Sepúlveda** **6/10/24 8:46:00 PM**

Page 28: [36] Deleted **Julio Sepúlveda** **6/10/24 8:52:00 PM**

Page 28: [37] Deleted **Sebastian Ignacio Cantarero** **5/5/24 10:17:00 PM**

Page 28: [38] Formatted **Julio Sepúlveda** **6/10/24 9:30:00 PM**

Outline numbered + Level: 1 + Numbering Style: Bullet + Aligned at: 0" + Indent at: 0.25"

Page 28: [39] Deleted **Edgart Flores Rafael** **6/17/24 8:31:00 PM**

Page 28: [40] Deleted **Sebastian Ignacio Cantarero** **6/14/24 9:31:00 PM**

Page 28: [41] Formatted **Julio Sepúlveda** **6/10/24 9:30:00 PM**

Font color: Black

Page 28: [42] Formatted **Julio Sepúlveda** **6/10/24 9:05:00 PM**

Font color: Black

Page 28: [43] Formatted **Julio Sepúlveda** **6/10/24 8:56:00 PM**

Font color: Black

Page 28: [44] Formatted **Julio Sepúlveda** **6/10/24 8:57:00 PM**

Font color: Black

Page 28: [45] Deleted **Sebastian Ignacio Cantarero** **6/8/24 5:23:00 PM**

Page 28: [46] Formatted **Julio Sepúlveda** **6/10/24 9:00:00 PM**

Font color: Black

Page 28: [47] Deleted **Julio Sepúlveda** **6/10/24 9:17:00 PM**

•

Page 28: [48] Formatted **Julio Sepúlveda** **6/10/24 8:59:00 PM**

Font color: Black

Page 28: [49] Formatted **Julio Sepúlveda** **6/10/24 9:08:00 PM**

Font color: Black